RECENT ADVANCES IN SELECTIVE FUNCTIONALIZATION OF THE QUINAZOLINE SCAFFOLD

DOI: http://dx.medra.org/10.17374/targets.2023.26.330

Thiago dos Santos, Gabriel de P. Bueno, Thais R. Arroio, Giuliano C. Clososki

Research Center for Natural and Synthetic Products, Faculty of Pharmaceutical Sciences of Ribeirão Preto, University of São Paulo, Av. do Café S/N, Ribeirão Preto, SP 14.040-903, Brazil (e-mail: gclososki@usp.br)

Abstract. *This chapter addresses recent advances in selective functionalization of the quinazoline core, which is present in various pharmacologically important molecules and in molecules that are interesting for materials chemistry. Comments on the selectivity control, reactivity, structural diversity, and usability of the protocols developed for obtaining compounds with relevant applications are provided. Reactions based on S_NAR, C–H functionalization, cross-coupling, selective metalation, flow chemistry, photochemistry, and electrochemistry are highlighted.*

Contents

1. Introduction

Heterocyclic systems are important in drug discovery and represent over 85% of all bioactive molecules.[1] In this scenario, more than 75% of the drugs approved by the FDA (The Food and Drug Administration) bear an *N*-heterocyclic ring,[2] with the quinazoline core being worthy of highlight. This core is a privileged scaffold that is found in pharmaceutically relevant molecules, such as the epidermal growth factor receptor (EGFR) inhibitors **1-3** (which act against tumors),[3] the antihypertensive agent prazosin **4**, the human adenosine A_3 receptor antagonist **5**,[4] the anti-Alzheimer's disease agent **6**,[5] and the antileishmanial derivative **7**[6] (Figure 1).

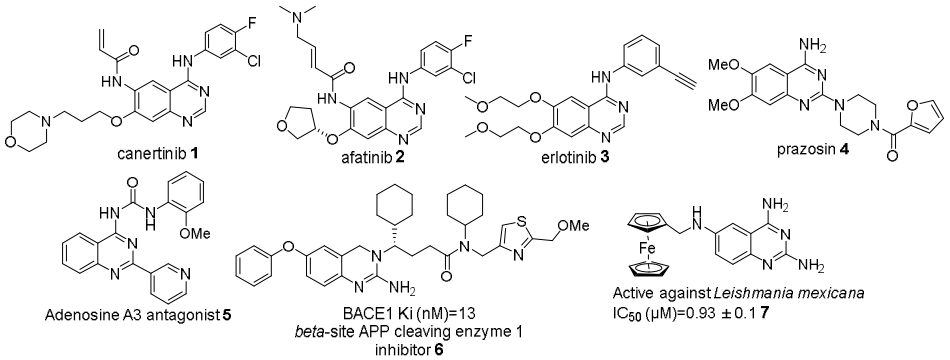

Figure 1. Examples of bioactive quinazolines.

Considering that the quinazoline core is widely explored for biologically active molecules, the development of selective protocols to obtain functionalized derivatives bearing this heterocycle is in great

demand. In this chapter, we discuss how functionalization of the quinazoline scaffold has advanced over the past eleven years (2012-2022) and comment on the selectivity, reactivity, chemical diversity, and synthetic application of quinazoline derivatives in the preparation of pharmaceuticals and other essential compounds.

2. Functionalization of the quinazoline scaffold

2.1. Nucleophilic aromatic substitution (S_NAr)

Nucleophilic aromatic substitution reactions have been commonly used to prepare numerous quinazolines. S_NAr selectivity and reactivity have improved considerably over the years. For example, in 2014 Vanelle and co-workers developed a selective amination protocol with **9** to functionalize 4-chloroquinazolines **8** under microwave irradiation to give the respective amino derivatives **10**. This approach serves as an alternative to the Buchwald-Hartwig cross-coupling reaction and allows less nucleophilic amines to be applied under DMAP (4-dimethylaminopyridine) catalysis (Scheme 1).[7]

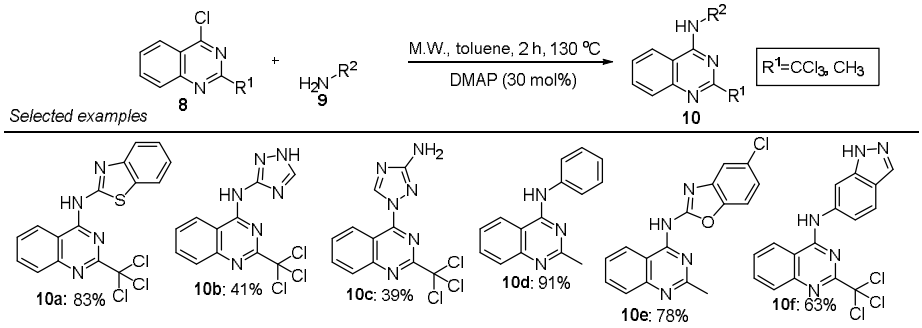

Scheme 1. DMAP-catalyzed S_NAr reaction for synthesis of 4-arylamino-2-substituted quinazolines.

The authors studied various heteroaryl amines and anilines, to obtain 45 functionalized quinazolines in reasonable to high yields (26-98%). Interestingly, when these authors used 3-amino-1,2,4-triazole, they obtained two products in 41 and 39% yield **10b-c**. Despite the presence of an electrophilic substituent (a trichloromethyl group) at position C2, selectivity at position C4 was maintained. Regarding the mechanism (Scheme 2), the *in-situ* generated cationic quinazoline intermediate **11** embraces substitution with the employed amine at position C4, to furnish the desired 4-aminoquinazoline; while catalyst **12** is regenerated.[7]

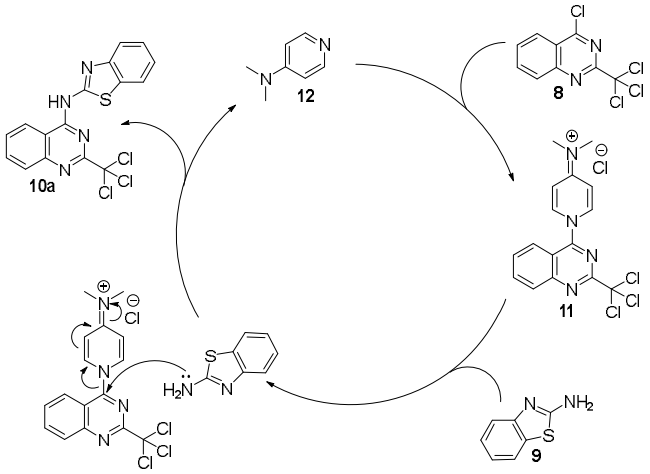

Scheme 2. Proposed mechanism for DMAP-catalyzed S_NAr reaction.

In 2017, Debache and co-workers described another efficient protocol for synthesizing a new class of 4-arylquinazoline hybrids. By using substrates with different electron-withdrawing or electron-donating groups, these authors allowed to react 2-quinolyl-4-chloroquinazolines **13** with substituted anilines **14**, to obtain twelve *N*-(4-heteroaryl)-2-(2-chloroquinolin-3-yl)quinazolin-4-amines **15** in moderate to good yields (48-75%) (Scheme 3). Under the optimal reaction conditions, HCl was the best catalyst in terms of selectivity and yield.[8]

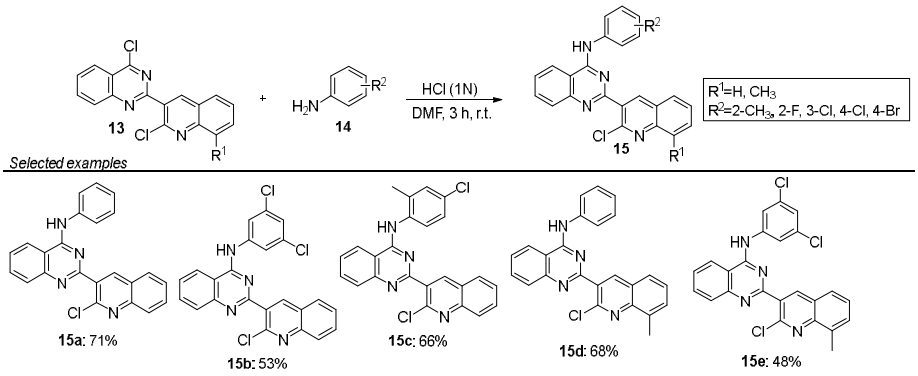

Scheme 3. HCl-Catalyzed S_NAr reaction for synthesis of 2-(2-arylaminoquinolyl)-4-arylaminoquinazolines.

In 2018, Tokiwa and co-workers used Breslow intermediates derived from different aldehydes **17** as acylating agents, to obtain direct nucleophilic alkanoylation of 4-chloroquinazoline **16**. The authors prepared and studied several Breslow intermediates, to obtain new 4-alkanoylquinazolines **18** (Scheme 4).[9] Although natural bond orbital (NBO) analysis shows that the π_{C-C} bond occupancy values of the Breslow intermediates and the reactivity for acylation are nearly correlated, the bulky nucleophiles arising *in situ* impede the reaction when intermediates with branched alkyl groups are employed. In the case of benzaldehydes with strong electron-withdrawing or strong electron-donating groups, the reaction uses the precursors on a non-catalytic scale.

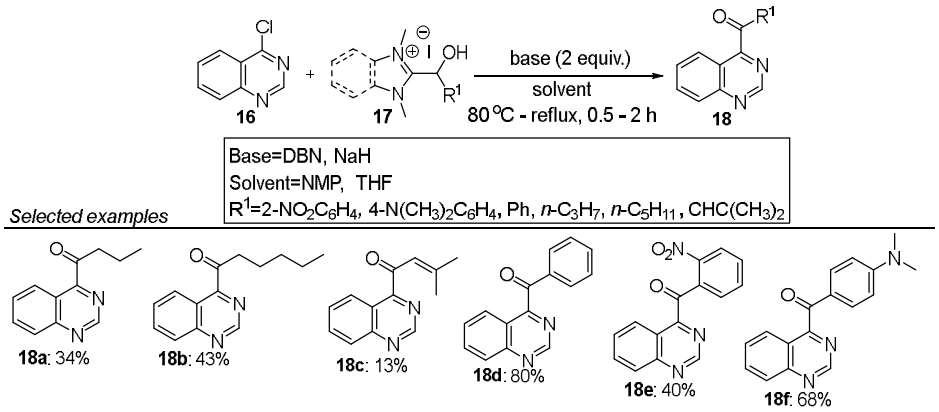

Scheme 4. Application of Breslow intermediates for synthesis of 4-alkanoylquinazolines *via* S_NAr.

In 2019, Liu and co-workers described direct Csp^2–H heteroarylation of the quinazoline scaffold under Brønsted acid catalysis with bis(trifluoromethanesulfonyl) imide (HTFSI) in hexafluoroisopropanol (HFIP) (Scheme 5). These authors applied the protocol to the quinazoline scaffolds of the first-generation EGFR

inhibitors erlotinib **21a-f** and gefitinib **21g-i**, which afforded compounds with potential kinase inhibition properties.[10]

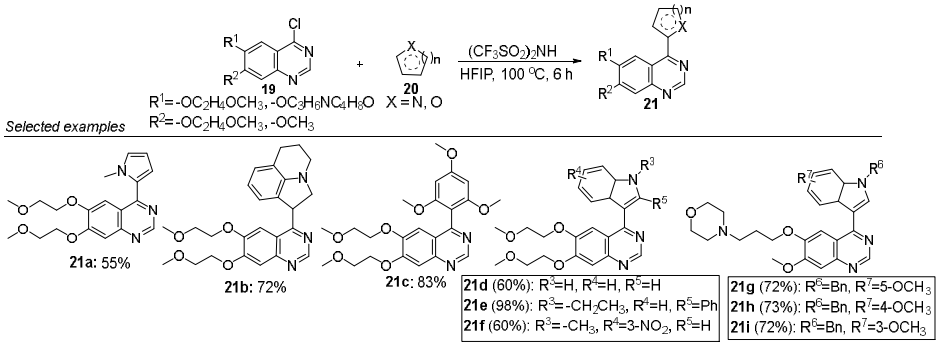

Scheme 5. Construction of 4-arylquinazoline derivatives *via* S_NAr/HFIP.

The reaction mechanism includes two possible pathways (Scheme 6). In Path A, HTFSI activates the C–Cl bond of 4-chloroquinazoline **19** *via* interaction between the hydrogen atom in HTFSI with the chlorine atom in **19**, to facilitate the nucleophilic substitution reaction with *N*-methylpyrrole **20**. Subsequent isomerization of **22** forms the desired product **23**. On the other hand, intermediate **24**, verified by NMR and HRMS in the presence or absence of HTFSI (Path B), would facilitate the *N*-methylpyrrole substitution reaction, followed by isomerization of **22** and subsequent formation of the same desired product.[10]

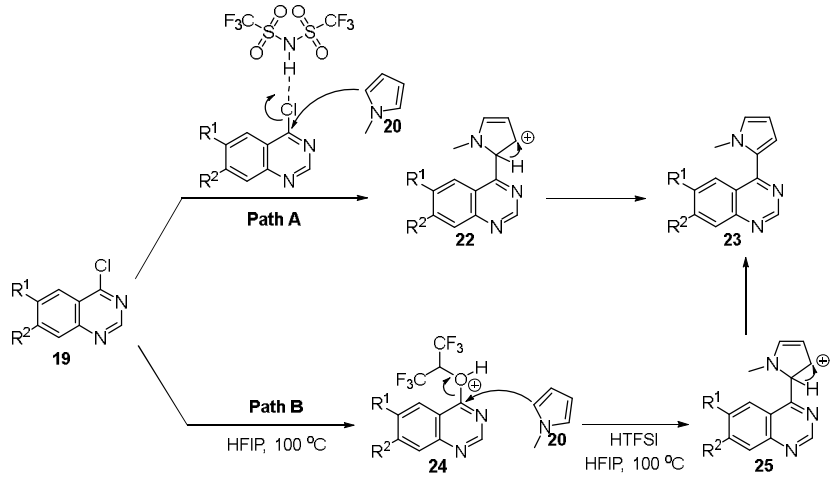

Scheme 6. Proposed reaction mechanism for direct Csp^2–H heteroarylation *via* two pathways.

In the same year, Nyalapatla and co-workers illustrated another selective acid-catalyzed S_NAr when they described a four-step synthesis of the epidermal growth factor receptor (EGFR) antagonist gefitinib **32** by employing 2,4-dichloro-6,7-dimethoxyquinazoline **26** as starting material with aniline **27**. The synthetic route furnished this drug in 4% overall yield on a gram scale comprising the selective demethylation of **28**, the *O*-alkylation of **29** with **30** under basic conditions, and the dehalogenation of **31**. Overall, the developed method, required inexpensive starting materials, and dismissed the need for chromatographic separations and protecting groups (Scheme 7).[11]

In 2021, Clososki and his research group described the microwave-mediated *N*-arylation of 4-chloroquinazolines **33**, as a fast, environmentally friendly, and efficient protocol that provided a library of

twenty nine 4-substituted anilinoquinazolines **35** including analogues of the antitumor agent verubulin in moderate to good yields (56-96%) (Scheme 8).[12] The established protocol demanded reduced amount of organic solvent, tolerated many *ortho*-, *meta*-, and *para*-substituted *N*-methylanilines and substituted anilines, **34** and, in contrast to previous literature,[13-16] did not require basic catalysis. The group assayed the biological potential of the obtained compounds against HCT-116 (human colorectal carcinoma), T98G (human glioblastoma), and MCF-7 (human breast adenocarcinoma) tumor cells, to find that **35a** is active toward the first two cell lines (IC_{50} values of 2.8 and 2.0 μM, respectively).[12]

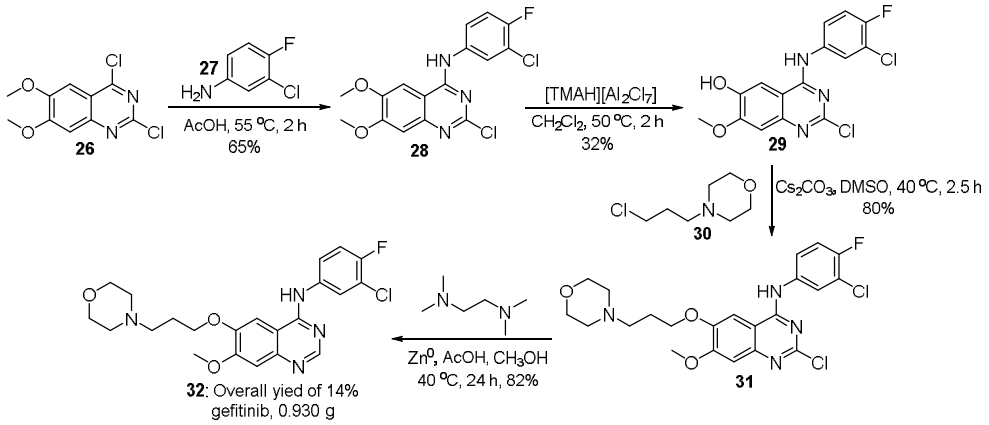

Scheme 7. 2,4-Dichloro-6,7-dimethoxyquinazoline as a new starting material for preparation of gefitinib.

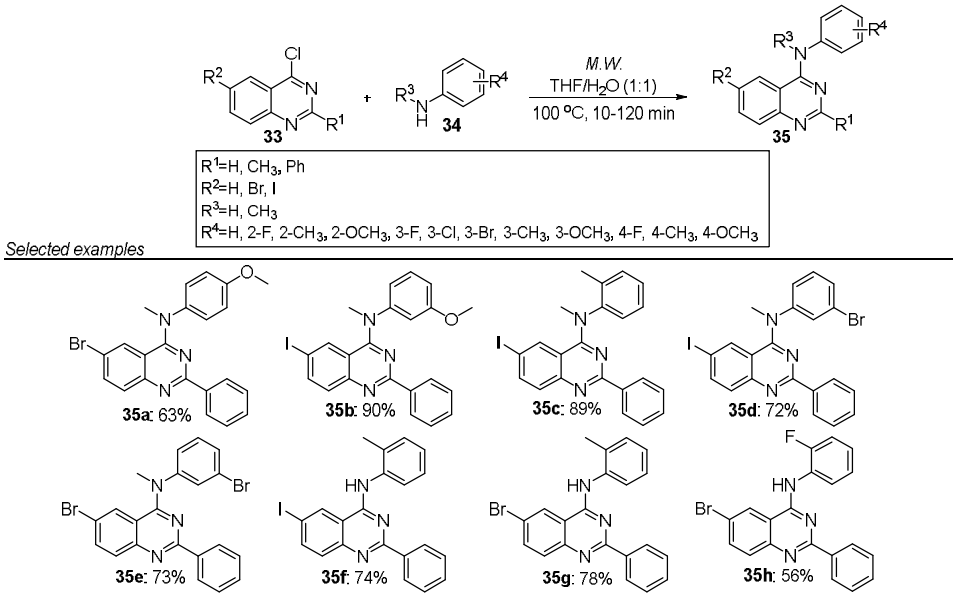

Scheme 8. *N*-Arylation reactions using 4-chloroquinazoline derivatives in a microwave reactor.

In 2021, Turks's research group reported the first example of synthetic studies on the preparation of 2-azido-4-alkyl/arylthioquinazolines **39** and 4-azido-2-alkyl/arylthioquinazolines **36** from **33** and their application in the synthesis of the corresponding 1,2,3-triazole derivatives (*e.g.* **37**, **39** and **40**). The group

employed an unusual sulfanyl group shift around the quinazoline core, which led to novel synthetic developments based on the leaving group capability of the azido group and the azidoazomethine-tetrazole tautomeric equilibrium (Scheme 9).[17]

By using S_NAr reactions with thiols at position C4 of quinazoline **36** (Scheme 9), Turks's research group prepared several derivatives **37** in moderate to good yields (51-83%). Subsequent treatment of the derivatives with sodium azide unusually shifted the sulfanyl group around the quinazoline core, allowing 5-(arylthio)tetrazolo[1,5-c]quinazolines **39** to be obtained: tautomerism of **38** gave a tetrazole that activates the system for a new S_NAr attack, but at position C2; the *in situ* formed ArylS- species acted as nucleophile.[17]

Turks's research group also investigated the regioselectivity of the acquired products by reversing the order of the S_NAr reactions. To perform such study, the group generated intermediate **41** from the reaction of quinazoline **36** with sodium azide, so that the tautomeric forms could activate position C2 while favoring substitution with sulfanyl at position C4 as in the case of **42**. Additionally, the group employed the azido tautomer **41** in a catalyzed 1,3-dipolar azide cycloaddition in the presence of an aliphatic or aromatic alkyne (*e.g.* **43a**), to find that its reactivity resembled the reactivity of fused 2-azidopyrimidines.[18-20] To complement these studies, Turks's research group explored the reactivity of **36** and **39** bearing an amine or alcohol group at position C2 or C4; the alkylthio substituent acted as leaving group (*e.g.* **37a**, Scheme 9). The substituted 1,2,3-triazolyl, known to be a leaving group, remained intact during transformation with the employed amine.[17]

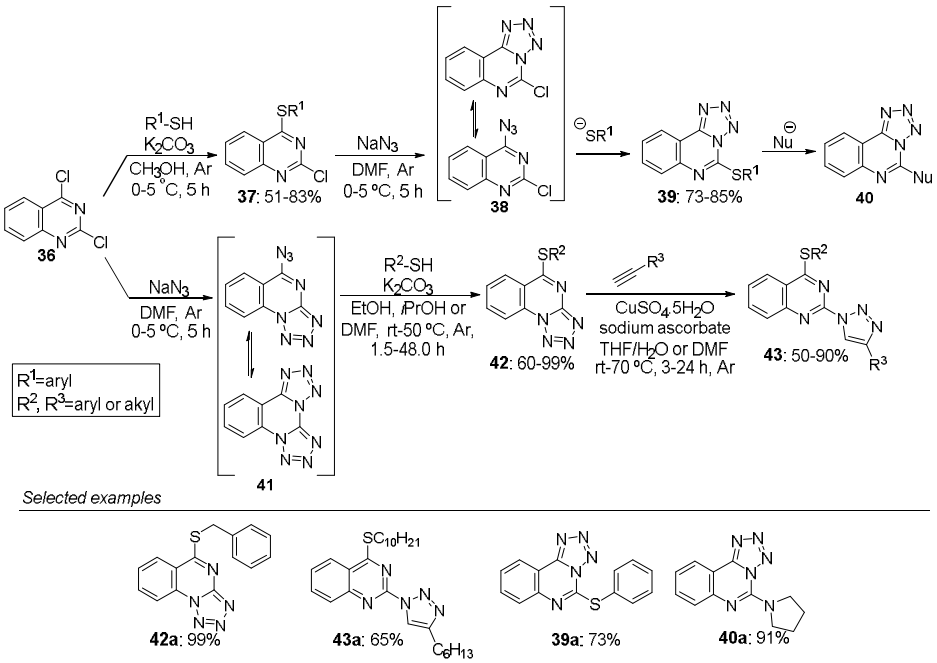

Scheme 9. Azide-tetrazole tautomerism and arylsulfanyl group shift during synthesis of thiosubstituted tetrazoloquinazolines.

In the same year, Turks's research group expanded the scope of this reaction by synthesizing new 2-amino-4-triazolylquinazolines **46** and 4-(alkyl/aryloxy)-2-triazolylquinazolines **49** bearing the triazole moiety at position C4 or C2 from **44** and **47** in the presence of **45** and **48**, respectively, while evaluating the robustness of tetrazolo[1,5-a]quinazoline substrates in CuAAC (Cu-catalyzed azide-alkyne cycloaddition reactions) (Scheme 10a-b). Furthermore, the group easily transformed the tetrazolo[1,5-a]quinazolines **50** into the corresponding 4-aminoquinazoline derivatives **52** by classic azide reduction (Staudinger reaction) while taking advantage of the high stability of the imino-phosphorane intermediate **51** against hydrolysis (Scheme 10c).[21-22] Some of the synthesized quinazoline derivatives showed promising photophysical properties, being

applicable in both fluorescent detection technologies and materials science. This was a remarkable achievement because the synthetic approaches allowed azido-tetrazole tautomerism to be applied to activate quinozaline rings for a C4- or C2-selective S_NAr reaction, not to mention that CuAAC reactions generate 2-(1*H*-1,2,3-triazole-1-yl)-4-(alkyl/arylthio)quinazolines in the presence of azido forms.[22]

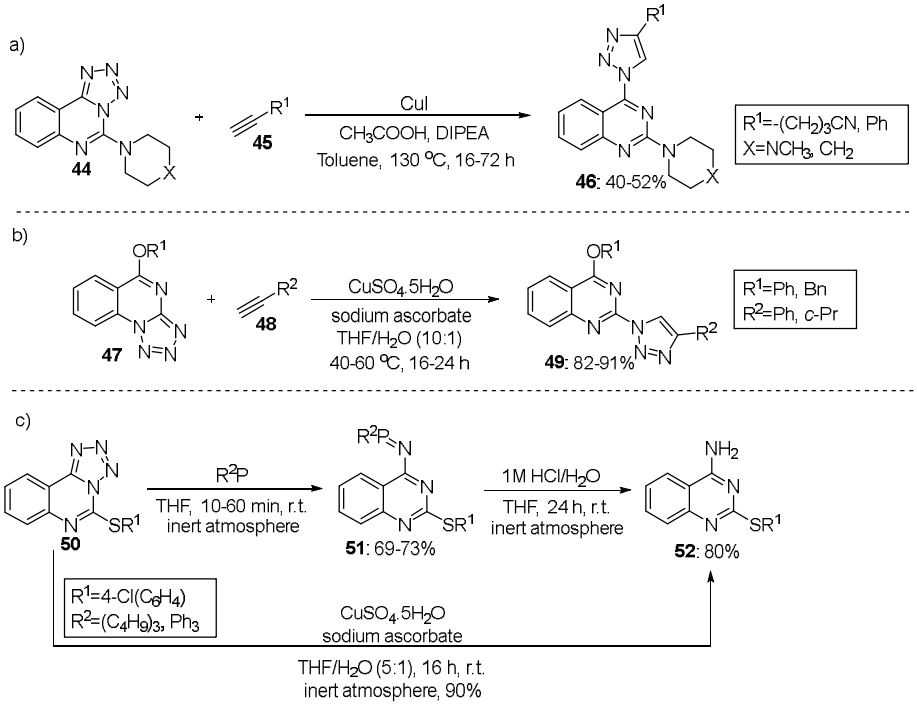

Scheme 10. Production of (a) 2-amino-4-triazolylquinazolines *via* CuAAC reactions, (b) 4-(alkyl/aryloxy)-2-triazolylquinazolines *via* CuAAC reactions, and (c) 4-aminoquinazoline derivatives by azide reduction.

In 2021, Witulski and co-workers investigated the photophysical properties of 2-*N*-aminoquinazolines **55** prepared *via* two consecutive S_NAr reactions, namely selective sodium methoxide-mediated substitution at position C4 of **53** followed by amination at position C2 of **54** (Scheme 11). The authors obtained 2-chloro-4-methoxyquinazolines **54** in 60-90% yield. Amines with different size and nucleophilicity were inserted at position C2 under reflux conditions, to give 2-amino-4-methoxyquinazolines **55** in 20-99% yield.[23] The authors investigated the prepared molecules in solution and in the solid state, along with cyclic voltammetry studies and computational studies to evaluate the HOMO/LUMO energy levels and the fluorescence-structure-charge distribution property (FSPR) relationship. The molecules can act as fluorescent probes that are responsive to the ambient, or they can be used as fluorophores in molecular recognition.[23]

In 2022, Mampa and co-workers established a synthetic route for producing the new quinazoline-based vascular endothelial growth factor receptor-2 (VEGFR-2) inhibitor **60**. This inhibitor had inhibitory concentration (Ki) of 0.15 µM, whereas vandetanib (a multi-kinase inhibitor) has Ki of 0.81 µM (Scheme 12).[24] The defined synthetic route started from 6-iodo-2-(4-methoxyphenyl)quinazolin-4(3*H*)-one **56**, which the authors subjected to halogenation with thionyl chloride, to obtain the 4-chloroquinazoline derivative **57** in DMF under reflux for 2 h. Subsequently, the authors reacted **57** with sodium ethoxide in ethanol (S_NAr, one-pot operation) under reflux for 2 h, to obtain 4-ethoxy-6-iodo-2-(4-methoxyphenyl)quinazoline **58**. Finally, a Suzuki-Miyaura cross-coupling reaction afforded 6-(3–chloro-4-fluorophenyl)-4-ethoxy-2-(4-

methoxyphenyl)quinazoline **60** after the authors employed 3-chloro-4-fluorophenylboronic acid **59** in the presence of $PdCl_2(PPh_3)_2$, (XPhos), and K_2CO_3, as base (Scheme 12).[24]

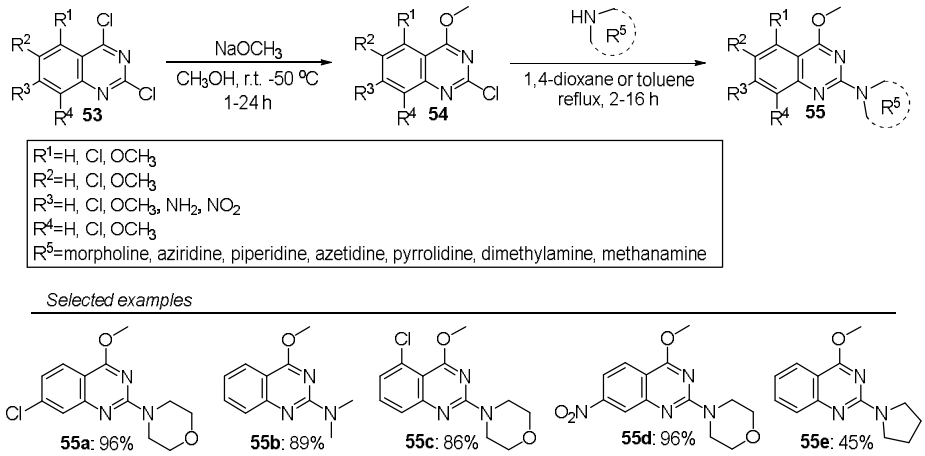

Scheme 11. Synthesis of 2-amino-4-methoxyquinazolines by side selective S_NAr reactions.

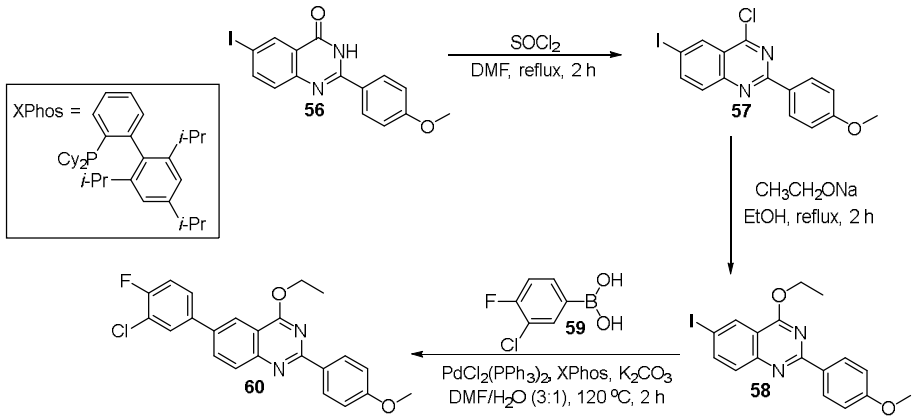

Scheme 12. Synthesis of 6-(3-chloro-4-fluorophenyl)-4-ethoxy-2-(4-methoxyphenyl)quinazoline.

When it comes to a more modern approach, flow chemistry is an innovative and widespread technology whose intrinsic characteristics facilitate and provide reproducible access to various chemical processes that would conventionally be problematic under batch conditions. This approach essentially consists of a stable set of conditions (activation/control), through which the reactants are passed.[25]

Djuric and co-workers took advantage of a continuous-flow protocol at high temperature and pressure, (Phoenix Flow Reactor™) to produce 2-aminoquinozaline derivatives **63** from 2-chloroquinazoline **61** and diverse nitrogen-based nucleophiles **62** *via* S_NAr (Scheme 13). 2-Aminoquinozalines are commonly found in pharmaceutical reagents, such as rosuvastatin and imatinib.[26] Although traditional protocols for synthesizing 2-aminoquinazolines exist, such protocols require adverse conditions of temperature and reaction time. An alternative is combining a robust continuous-flow system with statistical analysis *via* a DoE software (Design of Experiment), which provides an intelligent and efficient solution for obtaining such molecules. Djuric and co-workers evaluated reaction tests and monitored three variables: temperature, pressure, and flow. DoE analysis proved efficient, providing the ideal conditions of temperature (225 ºC), pressure (12 MPa), and flow

rate (0.5 mL/min), which afforded the product in 97% isolated yield. The protocol has been extended to various nitrogen-based nucleophiles, to give moderate to excellent yields (27-97%).[26]

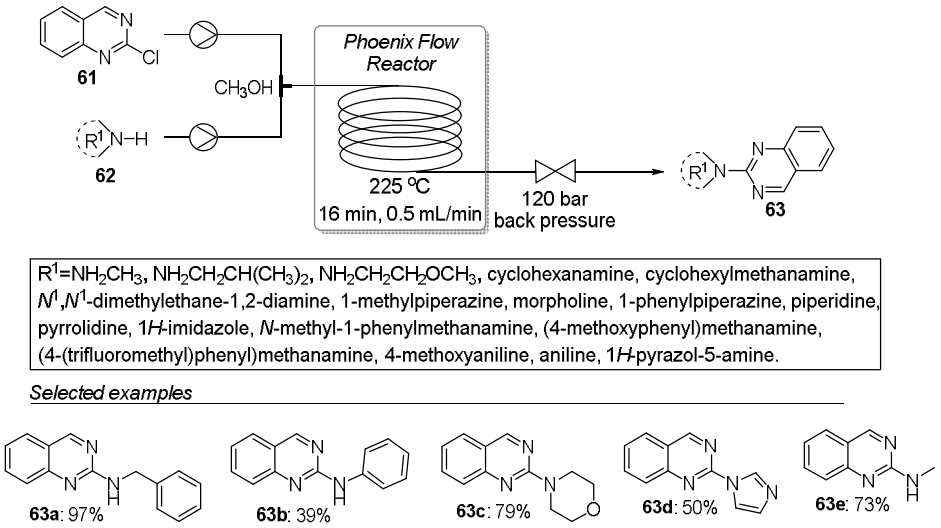

Scheme 13. Continuous-flow S_NAr between 2-chloroquinazoline and benzylamine.

2.2. C–H functionalization reactions

In recent years, C–H functionalization reactions catalyzed by or free of transition metals have reached remarkable versatility and sophistication. Today, these reactions represent a paradigm shift from the standard logic of synthetic chemistry, enabling advances in the construction of new scaffolds. In 2016, Zhang and co-workers explored Csp^2–H activation of **64** (Scheme 14) to develop a new protocol that allowed a series of benzimidazo[1,2-c]quinazolines **66a-f** to be synthesized *via* intramolecular cycloamination (mediated by $PhI(OAc)_2$ **65** as oxidant) in HFIP without any transition metals.[27]

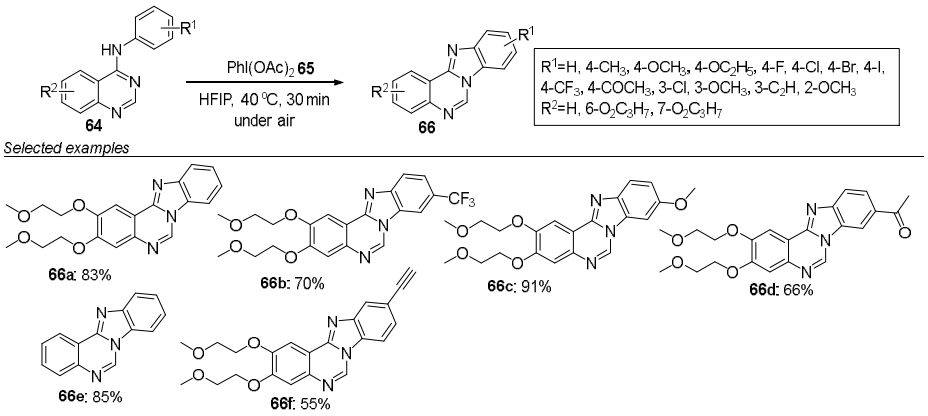

Scheme 14. C–H amidation of 4-anilinoquinazoline *via* $PhI(OAc)_2$.

By using 6,7-bis(2-methoxyethoxy)-*N*-phenylquinazolin-4-amine of type **64** as model substrate for C–H activation, Zhang and co-workers started to probe various reaction conditions. All experiments confirmed that $PhI(OAc)_2$ **65** was needed for synthesizing the desired product, and that highly polar solvents such as

HFIP, with high ionizing power and weak nucleophilicity, had to be used, to increase the final yield. The method is robust and versatile, as proven when the authors used several 4-anilinoquinazolines **64** bearing different electron-donating and electron-withdrawing groups. The reaction afforded the desired products with high regioselectivity control and can be used on a large scale, yielding conversions of 88% on a scale of 20 mmol.[27] Zhang and co-workers outlined a plausible mechanism (Scheme 15),[27] suggesting that the electrophilic *N*-iodine species **67** is formed from **64** with **65**, as a starting point. In the subsequent steps, there is electrophilic annulment of the pyridine nitrogen through cleavage of the N-I bond, to give a new intermediate **68**. The latter undergoes deprotonation, to afford the desired product **66**.

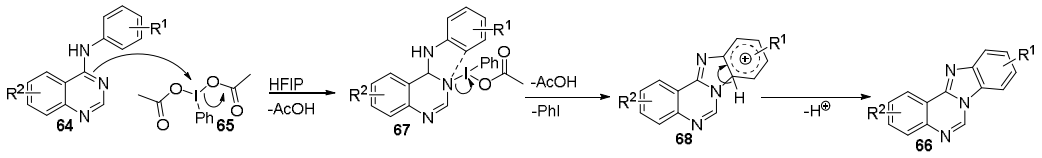

Scheme 15. Plausible mechanism of C–H amidation by $PhI(OAc)_2$.

Transition metal-free conditions in C–H functionalization reactions have attracted increasing attention, especially because they are inexpensive and do not generate toxic waste generation. In 2018, Peng's research group described alkylation of quinazoline-3-oxides **69** *via* radical oxidative coupling mediated by *tert*-butyl hydroperoxide (TBPB) and ethers such as **70** in moderate to good yields (15-82%) affording **71** (Scheme 16).[28] Given that the *N*-oxide fraction in the aza-heteroarene acts as a good *ortho*-directing group, Peng's research group used it as model in the cross-coupling of quinazolines, to obtain consecutive Csp^3–H/Csp^2–H bond functionalization. The group optimized many reaction parameters, to find that the best conditions were TBPB (1.0 equiv., as oxidant), inert atmosphere, 100 °C, and 4.5 h.[28]

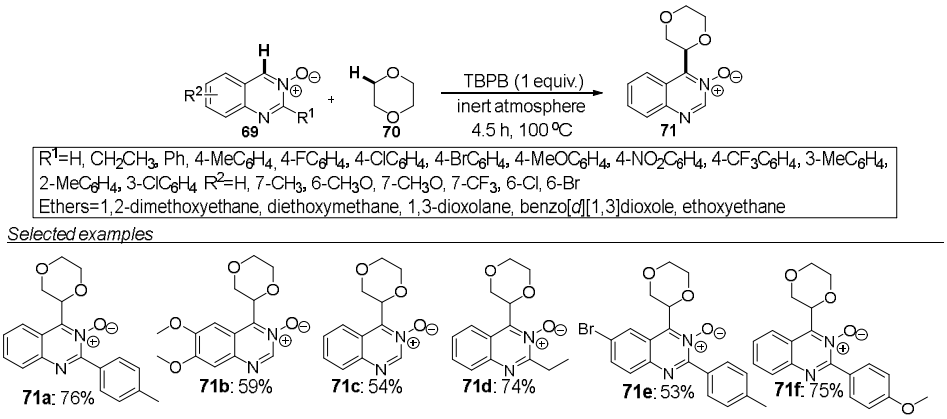

Scheme 16. Cross-coupling of quinazoline-3-oxide with 1,4-dioxane by TBPB.

Scheme 17 depicts a plausible mechanism for this reaction.[28] Initially, two radicals, **73** and **74**, originate from TBPB **72** decomposition. As evidenced by control experiments, radical **74** abstracts Csp^3–H from the ether **70**, to generate radical **75**, which readily reacts with quinozaline-3-oxides **69**, while radical **73** abstracts Csp^3–H from the formed species **76**. In the control experiment with di-*tert*-butyl peroxide (DTBP), the reaction was terminated because the *tert*-butoxyl radical **74** cannot abstract hydrogen atoms from species **76**.

In 2019, Peng's research group also explored the *N*-oxide **77** in the aza-heteroarene system in the presence of indoles **78** to synthesize 4-(indole-3-yl)quinazolines **79** *via* copper-catalyzed cross-dehydrogenative coupling (Scheme 18).[29] The group synthesized 4-(indole-3-yl)quinazolines derivatives **79** by employing the optimal reaction conditions: $CuCl_2$ (10 mol%, as a cheap catalyst) and oxygen (as oxidant) in methanol at 60 ºC.

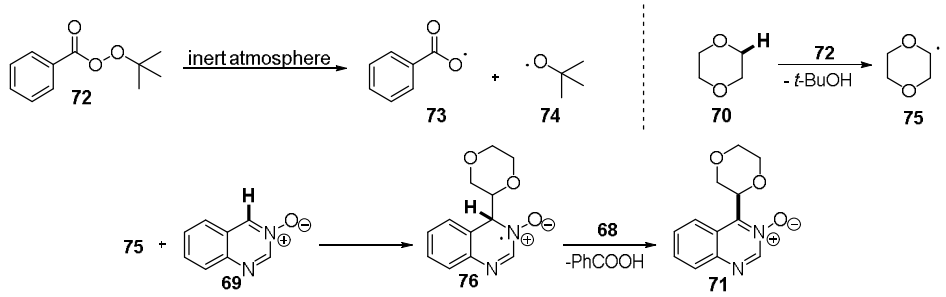

Scheme 17. Plausible mechanism for direct C4 alkylation of quinazoline-3-oxides.

Peng's research group evaluated the generality of this methodology by reacting indole derivatives **78** and quinazoline-3-oxides **77**. When an aryl group was the substituent at position C2 of the quinazoline moiety, electron-donating and electron-withdrawing groups on the ring affected the reaction slightly. On the other hand, strong electron-withdrawing substituents, such as the nitro group, retarded the reaction, to give the product **79b** in 61% yield only. The group also investigated substituents on the phenyl ring portion of quinazoline-3-oxide as for **79c**. Methyl, methoxy, trifluoromethyl, chlorine, and bromine were tolerated (52-84% yield), proving that the methodology is robust (Scheme 18).

When the group tested substituted indoles **78**, they obtained good yields. *N*-methylindoles bearing alkyl, halide, and alkoxy substituents at position C5 tolerated the reaction conditions (69-87% yield). Moreover, 1*H*-indole, *N*-benzylindole and *N*-isopropylindole showed good tolerance (82-88% yield). The presence of a methyl group at position C2 of indole conferred steric hindrance that influenced the reaction outcome (58% yield). However, indoles containing electron-withdrawing *N*-protecting groups (*N*-tosylindole) were not suitable for this transformation and were not detected (Scheme 18).

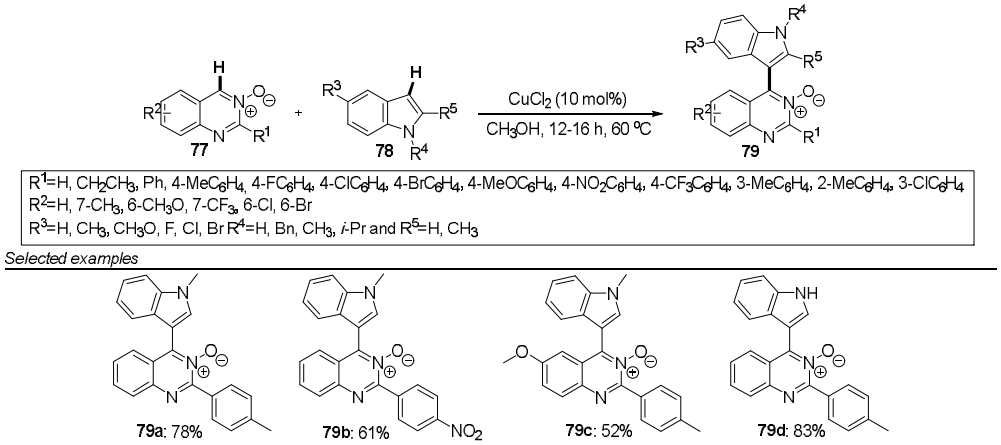

Scheme 18. Copper-dehydrogenative coupling of quinazoline-3-oxide with indoles.

The group performed experiments, to propose a plausible mechanism (Scheme 19).[29] $CuCl_2$ reacts with quinazoline-3-oxide **77**, to form intermediate **80** *via* C–H activation. This intermediate undergoes oxidative insertion at position 3 of indole **78**, to afford **81**. Next, a disproportionation oxidation affords the Cu(III) complex **82** with a second equivalent of $CuCl_2$, releasing CuCl. Finally, reductive elimination gives the product 4-(indole-3-yl)quinazoline **79** and Cu(I) species, which is reoxidized to $CuCl_2$ by O_2 and HCl.

In the same year, Savage and co-workers developed a new method to activate C–H by using picolyl amines as directing group for selective arylation at position C5 of the quinozaline core **83**. This allowed

efficient synthesis of 5-(5-phenyl-4-((pyridin-2-ylmethyl)amino)quinazolin-2-yl)pyridine-3-sulfonamide derivatives **84** as potent inhibitors of the enzyme IKur, a potential target when treating atrial arrhythmias (Scheme 20).[30] The established set of conditions included using $Pd(OAc)_2$ (5 mol%, as catalyst) with cesium pivalate in anisole at 120 ºC. Savage and co-workers expanded the reaction scope to other iodoarenes and (hetero)arenes of interest, to obtain high selectivity and moderate to good yields (46-86%). These authors did not fully elucidate the reaction mechanism, but C–H activation reaction was not sensitive to oxygen, so the reaction is believed to proceed through a Pd(II)/Pd(IV) cycle.[30]

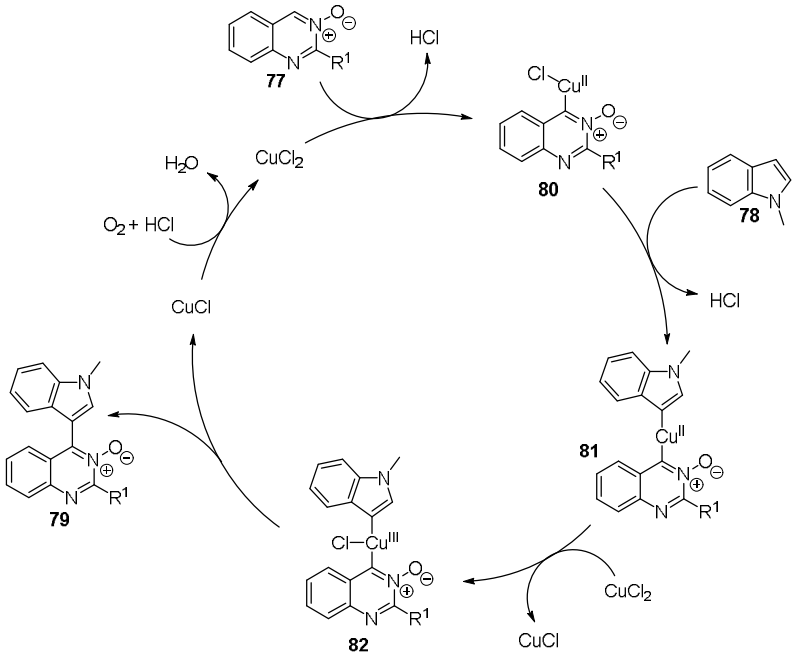

Scheme 19. Plausible mechanism for copper-dehydrogenative coupling of quinazoline-3-oxides.

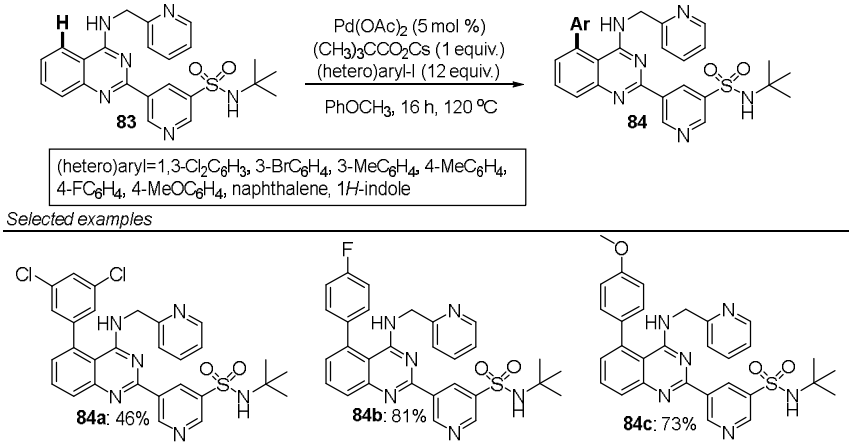

Scheme 20. Synthesis of selective IKur inhibitors *via* regioselective C–H arylation.

In 2020, Shiva Kumar and co-workers described a C–H *ortho*/*peri* selective functionalization/annulation by using substituted quinazolin-4-amines **85** with internal alkynes **86**. Through Csp^2–H activation of quinazolin-4-amine derivatives, this methodology provided pyridoquinazolines **87** in good yields (Scheme 21).[31] Under the optimized reaction conditions (reaction conducted in PEG-400 at 100 °C for 12 h), $RuCl_2$(*p*-cymene)$_2$ (5 mol%) and $Cu(OAc)_2{\cdot}H_2O$ (0.3 equiv.) proved to be the best catalytic combination in terms of selectivity and yield. The authors evaluated how different groups linked to the quinazoline scaffold influenced the reaction: for aniline moieties functionalized with electron-donating (4-CH_3 and 4-OCH_3, *e.g.* **87b**) and electron-withdrawing groups (4-Cl, 4-Br and CF_3, *e.g.* **87d**), *peri* C–H annulation reactions of *N*-phenylquinazolin-4-amines proceeded with high selectivity and good yields. The same happened when both electron-donating and electron-withdrawing groups were evaluated for internal alkynes (*e.g.* **87c**).. Furthermore, quinazolines with diverse substituents at positions C6 and C7 were well tolerated, resulting in moderate to good yields. They obtained 60% yield (1.08 g) when they evaluated a large-scale protocol.[31]

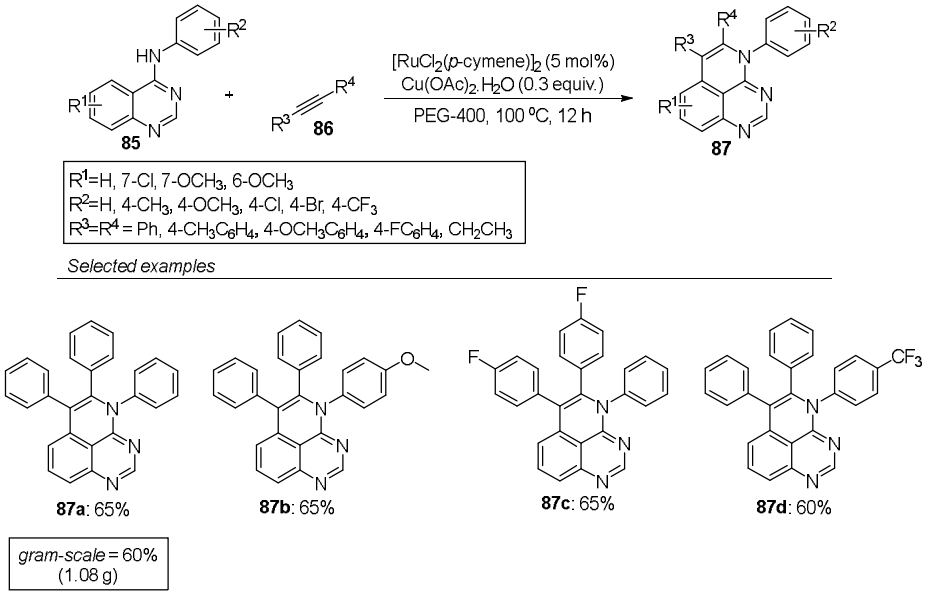

Scheme 21. Synthesis of triphenyl-4*H*-pyrido[2,3,4-*de*]quinazolines *via peri* C–H functionalization.

Shiva Kumar and co-workers proposed a plausible mechanism for the transformation. Catalysis begins with *in-situ* formation of the active catalyst $RuL(OAc)_2$ **89** through ligand exchange between $RuCl_2$(*p*-cymene)$_2$ **88** and acetate ions. Then, *peri* C–H activation of *N*-phenylquinazolin-4-amines **85** occurs, to furnish species **90**, which undergoes oxidative insertion of the alkyne **86** into the Ru-C bond, to give the ruthenium intermediate **91**. Finally, reductive elimination leads to the expected annulated product **87** and generates Ru^0 species, which is oxidized to Ru(II) by $Cu(OAc)_2{\cdot}H_2O$ (Scheme 22).[31]

In the same year, Chen's research group developed rhodium-promoted site-selective activation/annulation of quinazolin-4-amines **92** and diazo-compounds **93** in a one-pot cascade reaction protocol to afford quinazolines **94** (Scheme 23).[32] The methodology employed [Cp*$RhCl_2$]$_2$ (5 mol%), Ag_2CO_3 (0.3 equiv.), and 3-hydroxypivalic acid (as additive) and tolerated different substituents, including electron-donating and electron-withdrawing groups, at different positions of the aniline moiety. However, substrates with substituents at the *ortho*-position were little productive. Aliphatic substituents were tolerated in the protocol, affording moderate yields (23-50%), but bulky and cyclic substituents did not provide the desired products probably due to a steric effect. The group also evaluated diverse diazo compounds and identified limitation for cyclic ones.[32]

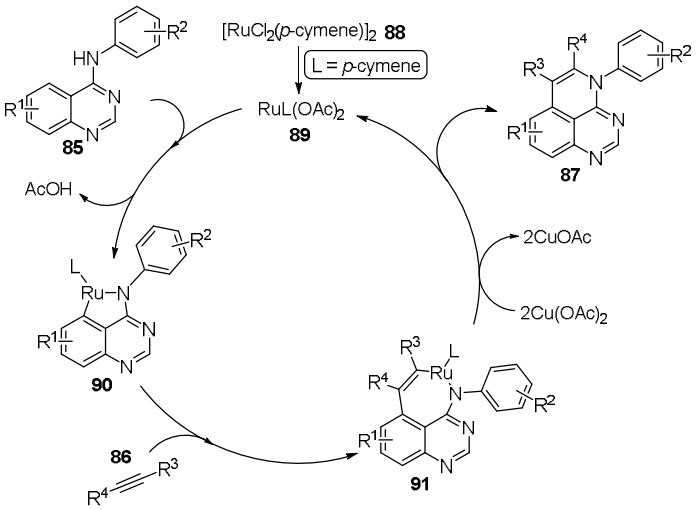

Scheme 22. Plausible mechanism of C–H activation with $RuCl_2$(*p*-cymene)$_2$.

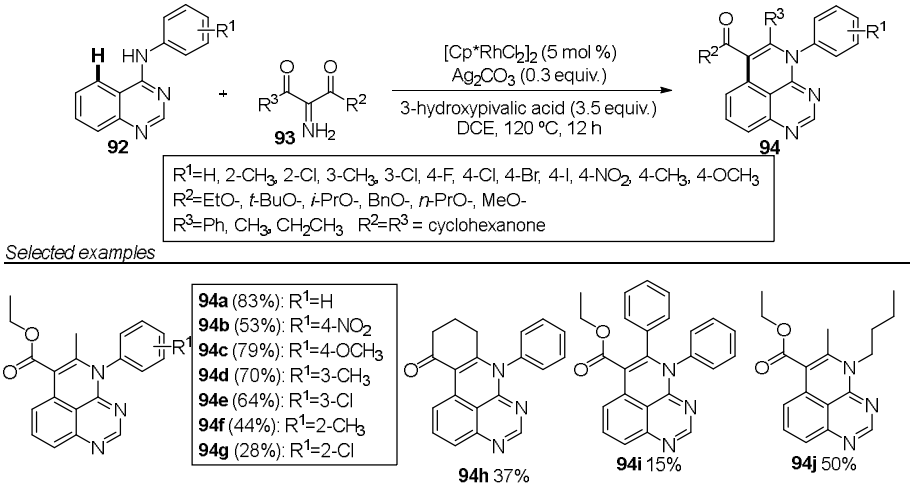

Scheme 23. Synthesis of fused 4-anilinoquinazolines *via* rhodium-catalyzed selective C–H bond activation.

Chen's research group carried out several control experiments to evaluate the mechanism and conceived the proposal in Scheme 24.[32] Rhodium coordinates with the *N*-atom of the aniline moiety from **92**, activating the Csp^2–H bond of the quinazoline core, to give species **95**. After the diazo compound **93** is added, **96** is obtained and converted into species **97** *via* migratory insertion. Then, intermediate **98** originates from protonolysis and undergoes further intramolecular cyclization, to afford the annulation product **94**.

In 2022, Cośkun and co-workers described the novel synthesis of 2,4-diarylquinazoline-3-oxides **101**, promoted by sustainable C–H functionalization catalysis of **99** with Mn(III) as oxidant in the presence of phenylboronic acids **100** (Scheme 25). These authors screened several boronic acids under the optimized conditions and obtained the desired Csp^2–H functionalization in good yields (70-83%). Neither electron-donating nor electron-withdrawing substituents gave parallel reactions, such as deoxygenation or rearrangement to quinazolin-4(3*H*)-one.[33] Concerning the mechanism (Scheme 26), it starts with homolysis of the C–B bond of **100** promoted by Mn(III), generating the aryl radical **102**, which adds to position C4 of

the quinozaline-3-oxide **99**, to generate the nitrogen-centered radical **103**. Then, an electron transfer from **103** to Mn(III) provides **104**. Finally, in the last step, deprotonation furnishes the expected product **101**.[33]

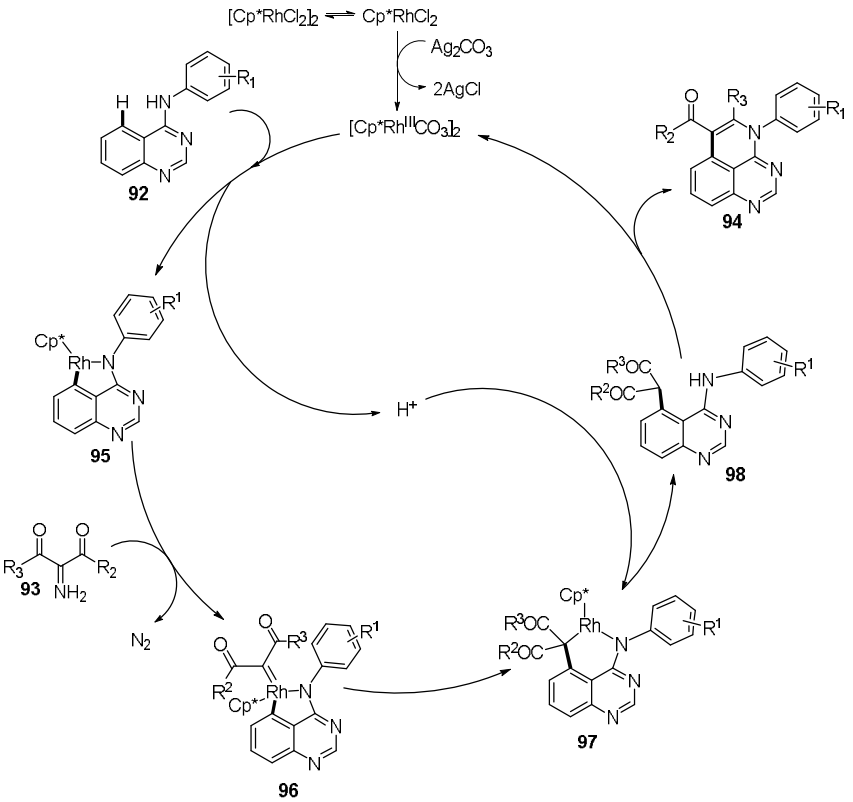

Scheme 24. Plausible mechanism of C–H activation with $[Cp^*RhCl_2]_2$ and Ag_2CO_3.

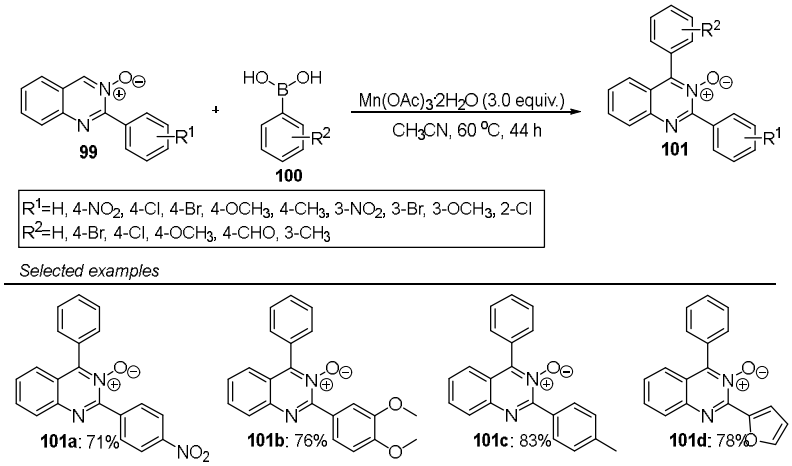

Scheme 25. Manganese-catalyzed C4 arylation of quinazoline-3-oxides with arylboronic acids.

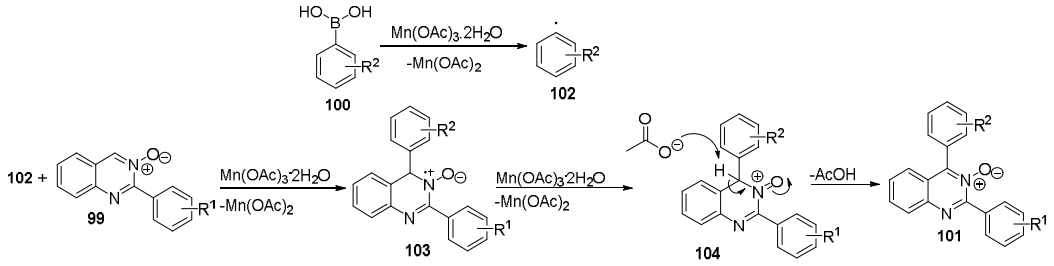

Scheme 26. A plausible mechanism for manganese-promoted arylation.

2.3. Cross-coupling reactions

Coupling reactions are important for constructing new C–C bonds, allowing different heterocycles, such as quinazolines, to be functionalized. In 2013, Peng's research group developed a methodology to obtain 4-CN-functionalized quinazolines **106** by reacting quinazoline-4-tosylates **105** with an inexpensive cyano source, copper(I) cyanide, in a reaction catalyzed by palladium (Scheme 27). Nitrile is a versatile group that can be directly converted to functional moieties, such as carboxyl, amide, amine, and aldehyde. Investigations showed that 2-substituted quinazolines bearing electron-rich aromatic systems were correlated with higher yields than 2-substituted quinazolines bearing electron-withdrawing aromatic systems. Additionally, some heterocycles including pyridine and furan were well tolerated.[34]

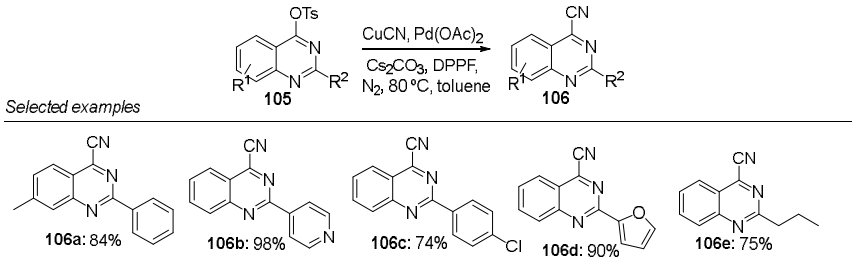

Scheme 27. Copper-catalyzed cyanation of quinazoline-4-tosylates.

Moreover, by adopting *N*-heterocyclic carbenes (NHC) **109** as ligands under co-catalysis by $Pd(PPh_3)_2Cl_2$ and CuI under mild conditions, Peng's research group explored C4-functionalization of quinazoline-4-tosylates **107** with terminal alkynes **108**, to obtain 4-alkynylquinazolines **110** (Scheme 28).[35]

In addition, Peng's research group investigated 4-OTs-quinazolines **111** to synthesize 2,4-diarylquinazolines **113** *via* nickel-catalyzed Kumada cross-coupling with different aryl Grignard reagents **112**. This protocol provided a straightforward route and another pathway to quinazolines functionalized at position C4, with yields varying from 64 to 88% (Scheme 29).[36]

In 2014, Wilson and co-workers demonstrated that it is possible to extend conjugation at position C6 of the quinazoline core as for **114** and to synthesize fluorescent kinase inhibitors **115** and **116** by using coupling reactions (Routes A and B) (Scheme 30). These probes can be modulated by substituent effects and the influence of conjugation. Several of the prepared compounds showed high fluorescence on-off while functioning as ERBB2 inhibitors against MCF7 tumor cells.[37]

Robin-Le Guen and co-workers provided another example of purposed-based and design-guided exploration of functionalization sites in this heterocyclic system *via* cross-coupling reactions. By means of Suzuki-Miyaura and Sonogashira reactions with **117**, these authors obtained quinazoline derivatives **118** and **119** with promising photophysical properties and potential direct application as colorimetric pH sensors in acidic medium (Scheme 31).[38]

Interestingly, Vanelle and co-workers synthesized 2,4,6,8-tetrasubstituted quinazolines **124** from 6,8-dibromo-2,4-dichloroquinazoline **120** *via* a practical, simple, and atom-economical one-pot

chemoselective approach consisting of sequential bis-S_NAr/bis-Suzuki-Miyaura reactions with **121** and **122** in the presence of **123**, respectively (Scheme 32).[39]

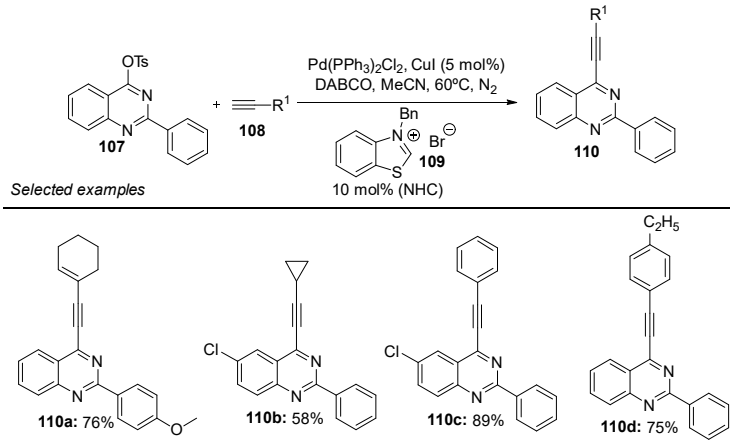

Scheme 18. Palladium- and copper-co-catalyzed preparation of 4-alkynylquinazolines from quinazoline-4-tosylates.

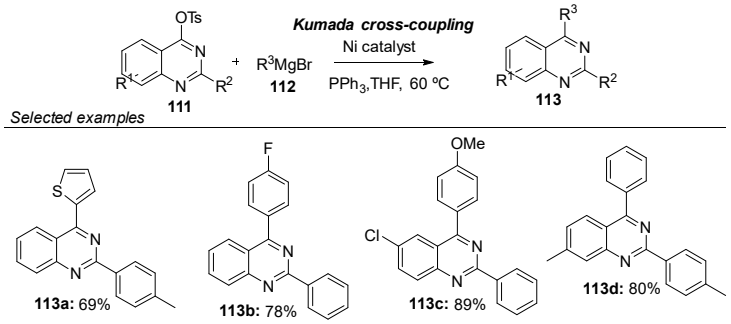

Scheme 29. Nickel-catalyzed Kumada-cross coupling of 4-OTs-quinazolines with Grignard reagents.

In 2015, Alami and co-workers described another palladium-catalyzed coupling reaction with 4-chloroquinazolines **126** and generated *N*-toluenesulfonylhydrazones from **125**. This allowed these authors to synthesize *iso*combretaquinazolines (*iso*CoQ) **127** which are analogues to *iso*combretastatin A-4 (*iso*CA-4) **128**, a known inhibitor of tubulin polymerization (Scheme 33). The authors evaluated how substitution of the trimethoxyphenyl ring for the quinazoline moiety influenced the activity, to find that some of the synthesized compounds at nanomolar level were active as anti-tubulin agents.[40]

To synthesize *N*-aryl-4[6-(2-fluoropyridin-3-yl)quinazolin-2-yl]-piperazine-1-carboxamides and -carbothioamides **132**, Kotakadi and co-workers considered a cross-coupling reaction as the key step (Scheme 34). These authors performed cyclization between 5-bromo-2-fluorobenzaldehyde **129** and guanidine carbonate in dimethylacetamide (DMA) followed by a Sandmeyer reaction, to obtain 6-bromo-2-iodoquinazoline **130**. This quinazoline was sequentially C2-substituted with piperazine, C6-arylated *via* a Suzuki-Miyaura reaction with **131** to afford **132**, and reacted with isocyanates and isothiocyanates, to provide the expected compounds **132** in good yields (73-82%). The authors assayed the antimicrobial properties of the compounds, to verify that electron-withdrawing groups such as fluor, chlorine, and trifluoromethyl on the ring gave the best bioactive candidates.[41]

In 2016, Peng's group gave an important scientific contribution by coupling organoindium compounds and 4-Ts-quinazolines **134** during one-pot C4-functionalization of the quinazoline core. Position C4 is vital

regarding kinase inhibitors such as gefitinib.[42] In previous works, application of 4-tosylquinazolines for coupling included arylboronic acids under palladium catalysis[43] or Grignard reagents through Kumada cross-coupling reactions,[36] but there were drawbacks like chemical incompatibility with limited scope for quinazoline scaffolding. However, the consolidated new protocol generated an extensive library of compounds **135** with functional group tolerance, in higher yields (Scheme 35).[42]

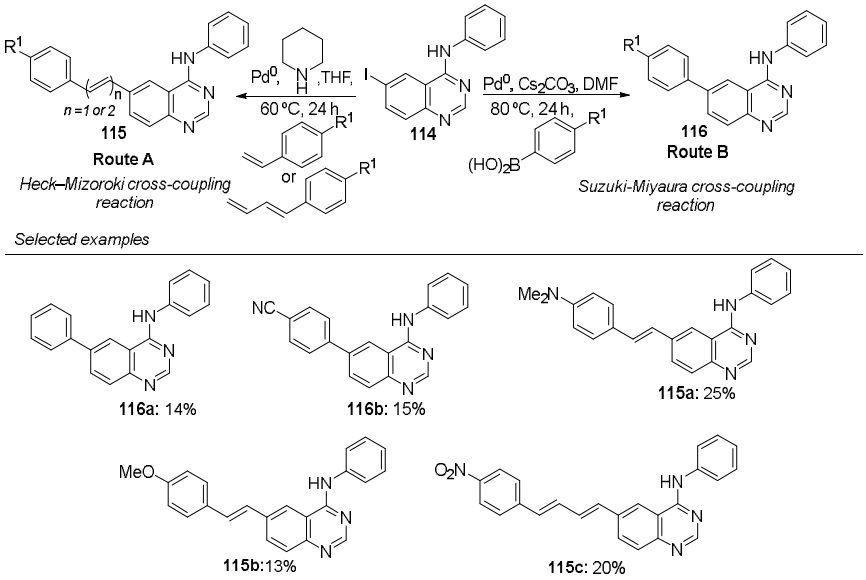

Scheme 30. Application of cross-coupling reactions at position C6 of the quinazoline core for preparation of kinase inhibitors.

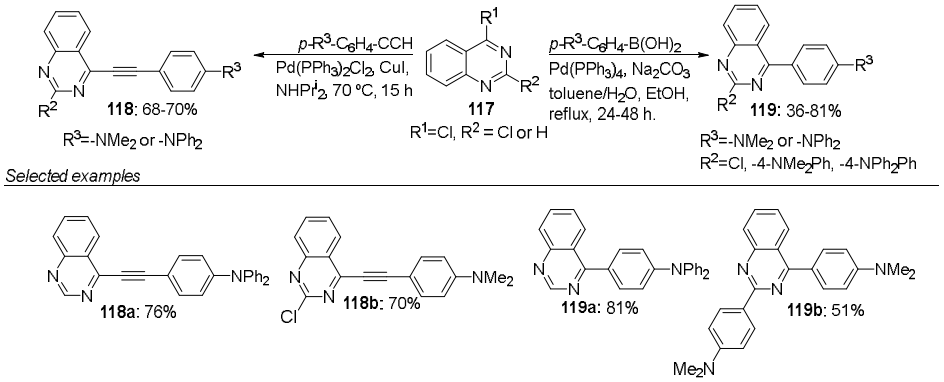

Scheme 31. Preparation of quinazolines displaying interesting photophysical properties.

In the following year, Iska and co-workers developed a methodology to produce 4-amino-2-arylquinazolines **138** from quinazolines bearing an unprotected NH_2 at position C-4 **136** *via* Suzuki-Miyaura coupling (Scheme 36). This allowed these authors to use different aryl and heteroaryl boronic acids **137** that were not suitable for the previous coupling approaches. The obtained compounds showed great antimicrobial activity, and one of them was more active than the standard antifungal Miconazole.[44]

In 2021, Rodríguez-López and co-workers used Suzuki-Miyaura coupling reactions between quinazolines **139** and diverse boronic acids **140** to generate compounds with promising photophysical

properties. These authors reported several *push-pull* 4-substituted and 4,7-disubstituted quinazolines **141** that exhibited strong emission in different solvents. Such emission was due to intramolecular charge transfer (ICT) and photoluminescence, in both the solid and solution state. The authors also studied how protonation affected these derivatives, to verify that fluorescence was quenched in some cases, and that new emission bands appeared in other cases (Scheme 37).[45]

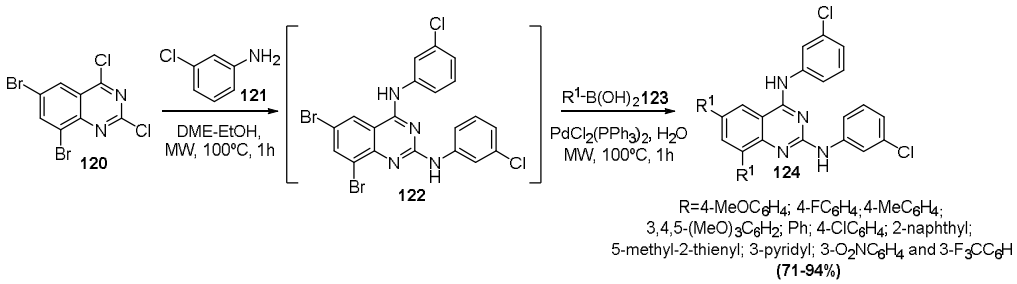

Scheme 32. One-pot preparation of tetrasubstituted quinazolines.

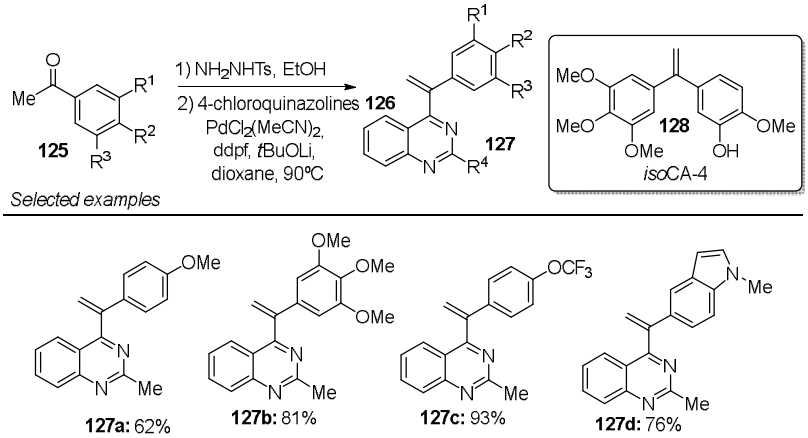

Scheme 33. Palladium-catalyzed coupling of 4-chloroquinazolines with prepared *N*-toluenesulfonylhydrazones.

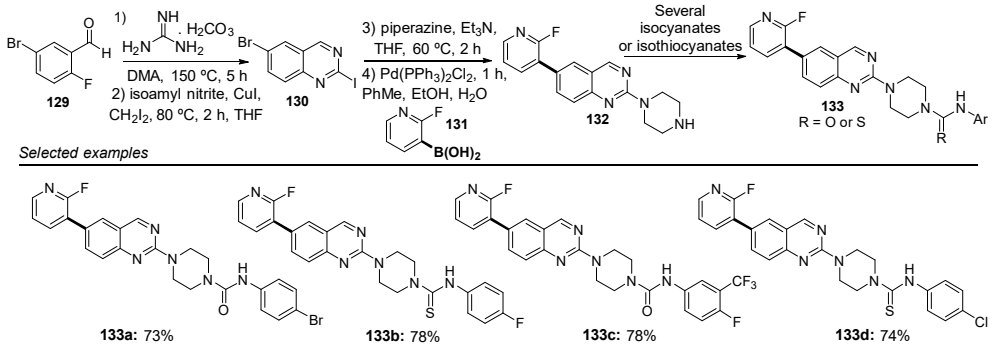

Scheme 34. Application of a Suzuki-Miyaura cross-coupling reaction to obtain *N*-aryl-4[6-(2-fluoropyridin-3-yl)quinazolin-2-yl]-piperazine-1-carboxamides and -carbothioamides.

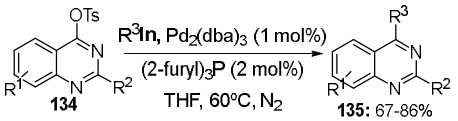

R^1=H, 7-Me, 5-F;
R^2=Ph, 2-MeC_6H_4, 3-MeC_6H_4, 2-MeC_6H_4, 4-MeC_6H_4, 4-OMeC_6H_4, 4-$Me_2NC_6H_4$,4-ClC_6H_4, 3-ClC_6H, 2-thienyl, 4-pyridyl, propyl, 2,5-$Cl_2C_6H_3$, 4-FC_6H_4, 4-$F_3CC_6H_4$;
R^3=R_2 and Me, Et, n-pentyl, isopropyl, cyclopropyl, cyclopentyl, (N-methyl)indol-2-yl, 5-methylfuran-2-yl

Scheme 35. Palladium-catalyzed coupling of organoindium with 4-tosylquinazolines.

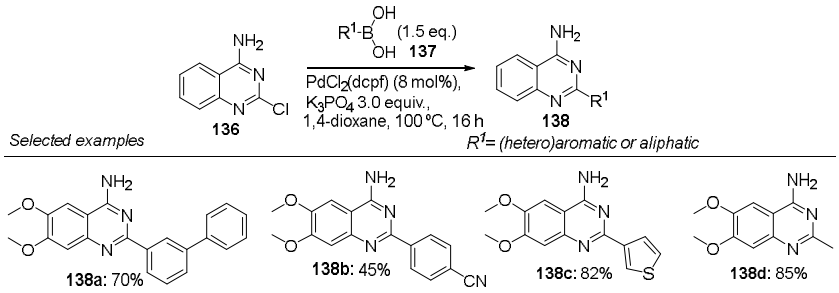

Scheme 36. The application of Suzuki-Miyaura coupling for 4-aminoquinazolines.

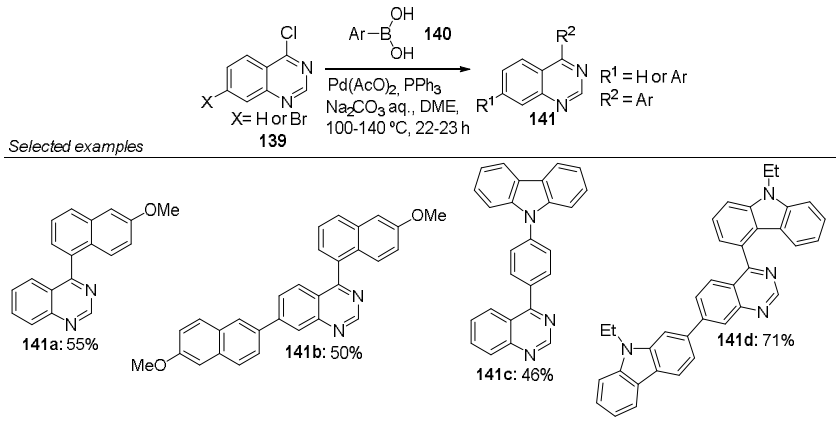

Scheme 37. Straightforward preparation of quinazoline chromophores *via* Suzuki-Miyaura coupling.

Drug resistance inspired the work developed by Patel and Rohit in 2021. Their work was based on the combination of different pharmacophores to obtain hybrids with potential antimycobacterial activity. These authors attached the quinazoline core, 1,3,4-thiadiazole, and piperazine including a S_NAr reaction of **142**, a Suzuki-Miyaura coupling to obtain **144** from **143** followed by the Mannich reaction of **145**, in order to obtain pharmacologically active derivatives **146** (Scheme 38).[46] Structure-activity relationship (SAR) studies demonstrated that substitutions at the *para* position of the phenyl ring of the piperazine-thiadiazoline-quinazoline hybrids influenced the antimycobacterial activity. The substituents -CF_3, -OH, or -Br were associated with better activity against M. *tuberculosis* H37Rv cells and very low cytotoxicity against human cervical cells (HeLa).[46]

Complementing the studies conducted by Peng's research group on C4-functionalization of quinazolines, in 2021 that same group investigated palladium-catalyzed coupling of 4-tosyloxyquinazolines **147** with indole-based systems **148**. The group established an efficient method with excellent functional group

tolerance, totalizing 29 4-(1*H*indol-1-yl)quinazolines of type **149** (41-98%) (Scheme 39). The anticancer relevance of quinazolines functionalized with *N*-heterocycles at position C-4 motivated the study.[47]

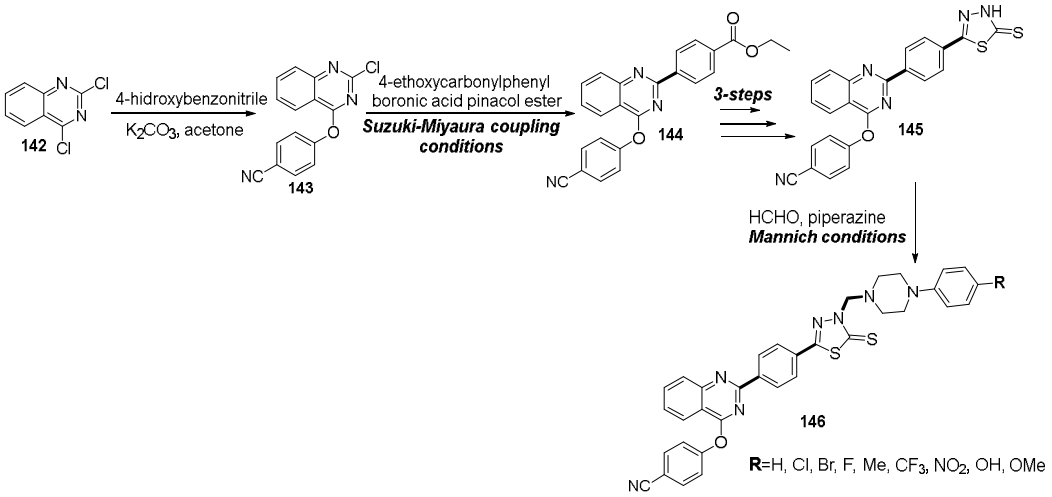

Scheme 38. Application of Suzuki-Miyaura coupling for preparation of antimycobacterial agents.

In addition, in 2022, Peng's research group developed a new approach based on a palladium-C-/P-H cross coupling reaction that used the same 4-OTs-quinazolines **147** but with **150** to synthesize novel 4-phosphorylated quinazolines **151** (52-99%) (Scheme 39). Organophosphorus compounds can serve as versatile building-blocks in organic synthesis, and quinazolines bearing this moiety are promising bioactive heterocyclic systems if we consider high activity reported for 3-phosphoindole derivatives against NNRTI-resistant HIV-1.[48]

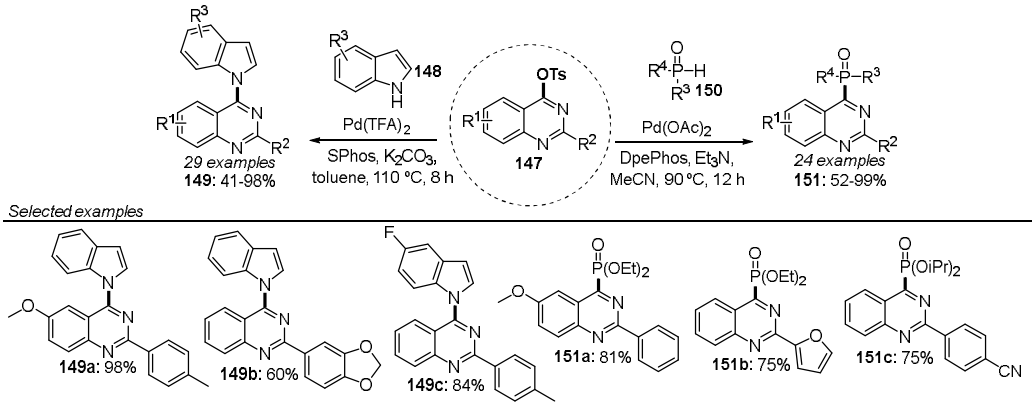

Scheme 39. The latest advances on the use of 4-tosyloxyquinazolines in coupling reactions.

2.4. Selective functionalization *via* metalation

Regioselective deprotometalation protocols involving the use of TMP-based bases (TMP=2,2,6,6-tetramethylpiperidyl) have found wide application in the functionalization of diverse aromatic and heterocyclic substrates.[49,50,51,52] Concerning the use of this approach in the case of the quinazoline skeleton, Clososki's research group applied an *in-situ* trapping strategy to metalate quinazoline **152**: pre-complexation of this substrate with $ZnCl_2$ in THF followed by addition of LiTMP promoted regioselective deprometalation

at position C8. The group further treated the metalated species with molecular iodine, to obtain the functionalized heteroarene **153** in 83% yield, that was then subjected to S_NAr to afford **154**, an analogue of the antitumor agent verubulin (Scheme 40).[53]

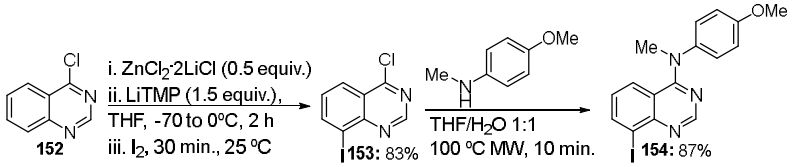

Scheme 40. Selective metalation of 4-chloroquinazoline and synthesis of a verubulin analogue.

2.5. Photocatalyzed reactions and electrochemical functionalization

The current interest in visible-light photoredox-catalyzed processes derives from the advantages of the reactions performed under such conditions, including the possibility of using visible light or sunlight as a renewable source, their suitability for generating highly reactive species in a mild and controlled way, and their great tolerance to functional groups.[54,55] Similarly, organic electrosynthesis is environmentally friendly and minimizes or eliminates waste generation during the reactions. Furthermore, electrochemical protocols can be easily scaled up for industry settings and may give valuable side products like hydrogen gas.[56]

With respect to functionalization of the quinazoline system, Wacharasindhu and co-workers applied Rose Bengal as a nonhazardous and inexpensive photocatalyst under visible light to promote amination of 4-mercaptoquinazoline **155** with different amines, to afford 4-aminoquinazolines **156a-c** in good yields (Scheme 41).[57]

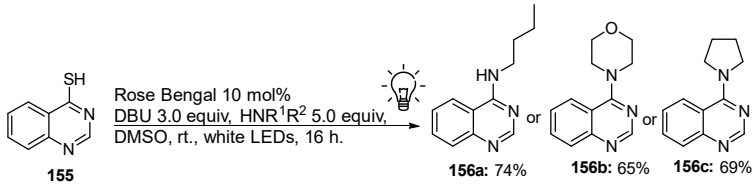

Scheme 41. S_NAr of 4-mercaptoquinazoline under visible light.

In 2017, Helaja and co-workers employed ascorbic acid, both as sacrificial reductant and Bronsted acid, with $Ir[dF(CF_3)ppy]_2(dtbbpy))PF_6$ under blue light to debenzylate quinazoline **157** selectively, to obtain quinazolinone **158** in excellent yield in 2 h (Scheme 42).[58]

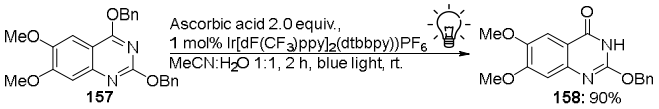

Scheme 42. Selective iridium-catalyzed removal of a *O*-benzyl group under blue light.

By employing the same photocatalyst ($Ir[dF(CF_3)ppy]_2(dtbbpy))PF_6$) under blue light irradiation in the presence of trifluoroacetic acid (TFA) and *tert*-butyl peracetate (*t*-BPA, as oxidant) in dimethyl sulfoxide for 24 h, Wang and co-workers selectively coupled quinazoline **159** with *N*-Boc-pyrrolidine **160** when they prepared the aminoalkylated derivative **161** in 40% yield (**S**cheme 43A).[59] Under similar conditions, the same electrophilic position of **159** can be functionalized with cyclohexyl iodide[60] **162** or bromocyclohexane[61] **164** during synthesis of alkylated quinazolines **163** and **164** in 36 and 56% yields, respectively (Scheme 43B-C).

As for electrochemical functionalization of the quinazoline scaffold, Pan and co-workers developed an interesting approach that used carbazate **166** as an alkyl radical surrogate *via* electrochemical anodic oxidative fragmentation with **159**. The protocol employed platinum/graphite electrodes in an undivided cell,

n-Bu_4NClO_4 as electrolyte, and constant current of 3 mA in a DMSO/MeCN 1:1 mixture for 14 h, to obtain the alkylated quinazoline **167** in 68% yield (Scheme 43D).[62]

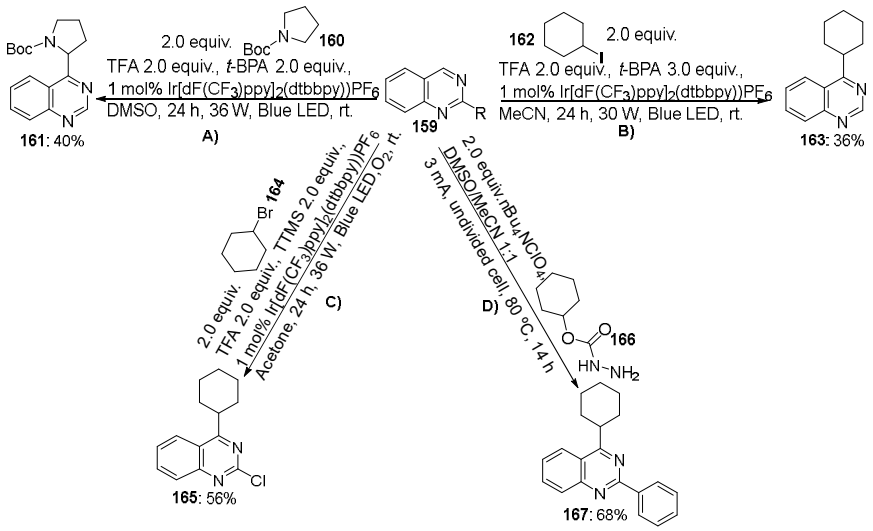

Scheme 43. Photoredox and electrochemical alkylation of quinazolines.

Boyd and co-workers developed an innovative method to couple 7-bromo-2-methylquinazoline **168** with potassium alkyl trifluoroborates **169** *via* nickel/photoredox dual catalysis under continuous flow in the preparation of quinazolines **170** (Scheme 44).[25] The authors evaluated solutions to the problems obtained in conventional batch photochemical reactions, which generally are not suitable in a medicinal chemistry environment (poor control of parallel reactions of interest) and present issues of inefficient irradiation, difficult scale-up, and poor refrigeration. In addition, process sensitivity to oxygen makes it operationally difficult. Thus, these authors developed a simple methodology for Csp^3–Csp^2 coupling that involved significantly shorter reaction times, a wider scope of **170** (19-58% yield), and possibility of scale-up. The best conditions were LED (450 nm) with power of 24 W, flow rate of 250 μL/min, 40 min, [Ir{dFCF$_3$ppy}$_2$(bpy)]PF_6 (3 mol%, as catalyst), $NiCl_2$·dme/dtbbpy (12 mol%, as ligand), and 1:4 DMA/dioxane (as solvent mixture), which guaranteed total solubility of the substrates (Scheme 44).[25]

3. Conclusions

Over the last decade, the importance of the quinazoline system in bioactive compounds such as pharmaceuticals and in molecules with attractive photophysical properties for application in materials chemistry (*e.g.* quinazoline-based chromophores) has been attracting a great deal of attention from synthetic organic and medicinal chemists. Obtaining high structural diversity by using selective protocols that target the quinazoline core instead of constructing a substituted core has driven innovation in this field and is a current demand.

Although most approaches over the past years have concentrated efforts on functionalizing position C4 (*e.g.* new catalyzed S_NAr reactions), great progress has been made toward functionalizing positions C2, N3, and C5–C8 by employing diverse catalytic systems or different directing groups.

Regarding emerging and modern synthetic strategies in organic synthesis, few papers on photocatalysis and electrosynthesis have been published for this heterocycle so far. Therefore, there are great opportunities of work in this area to address scarcely investigated positions *via* selective functionalization strategies.

In summary, the quinazoline ring is a privileged system with various applications, and its direct functionalization still has room for further developments while accumulated knowledge about its reactivity in terms of electrophilicity and nucleophilicity and how to modulate these properties cannot be disregarded.

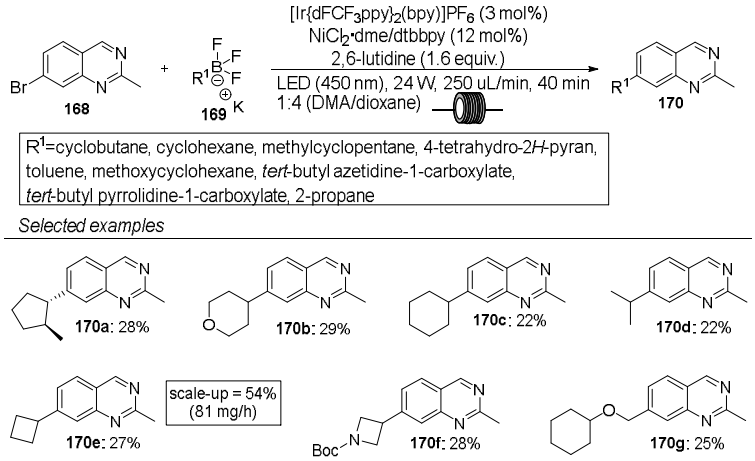

Scheme 44. Continuous-flow nickel/photoredox-catalyzed coupling of 7-bromo-2-methylquinazoline with potassium alkyl trifluoroborates.

Acknowledgements

The authors thank CNPq (140137/2018-1 and 163350/2021-3), CAPES, and FAPESP (grant 2020/13962-9).

References

1. Heravi, M. M.; Zadsirjan, V. *RSC Advances* **2020**, *10*, 44247-44311.
2. Kerru, N.; Gummidi, L.; Maddila, S.; Gangu, K. K.; Jonnalagadda, S. B. *Molecules* **2020**, *25*, 1-42.
3. Das, D.; Hong, J. *Eur. J. Med. Chem.* **2019**, *170*, 55-72.
4. Jia. F.-C.; Zhou, Z.-W.; Xu, C.; Cai, Q.; Li, D.-K.; Wu, A.-X. *Org. Lett.* **2015**, *17*, 4236-4239.
5. Haghighijoo, Z.; Zamani, L.; Moosavi, F.; Emami, S. *Eur. J. Med. Chem.* **2022**, *227*, 113949.
6. Mendoza-Martínez, C.; Galindo-Sevilla, N.; Correa-Basurto, J.; Ugalde-Saldivar, V. M.; Rodríguez-Delgado, R. G.; Hernández-Pineda, J.; Padierna-Mota, C.; Flores-Alamo, M.; Hernández-Luis, F. *Eur. J. Med. Chem.* **2015**, *92*, 314-331.
7. Gellis, A.; Kieffer, C.; Primas, N.; Lanzada, G.; Giorgi, M.; Verhaeghe, P.; Vanelle, P. *Tetrahedron* **2014**, *70*, 8257-8266.
8. Derabli, C.; Boulcina, R.; Kirsch, G.; Debache, A. *Tetrahedron* **2017**, *73*, 351-358.
9. Suzuki, Y.; Iwata, N.; Dobashi, K.; Takashima, R.; Arulmozhiraja, S.; Ishitsubo, E.; Matsuo, N.; Tokiwa, H. *Tetrahedron* **2018**, *74*, 392-400.
10. Yuan, S.; Yu, B.; Liu, H.-M. *Adv. Synth. Catal.* **2019**, *361*, 59-66.
11. Maskrey, T. S.; Kristufek, T.; Laporte, M. G.; Nyalapatla, P. R.; Wipf, P. *Synlett* **2019**, *30*, 471-476.
12. Nishimura, R. H. V.; Dos Santos, T.; Murie, V. E.; Furtado, L. C.; Costa-Lotufo, L. V.; Clososki, G. C. *Beilstein J. Org. Chem.* **2021**, *17*, 2968-2975.
13. Xu, P.; Chu, J.; Li, Y.; Wang, Y.; He, Y.; Qi, C.; Chang, J. *Bioorg. Med. Chem.* **2019**, *27*, 114938.
14. Choudhary, S.; Doshi, A.; Luckett-Chastain, L.; Ihnat, M.; Hamel, E.; Mooberry, S. L.; Gangjee, A. *Bioorg. Med. Chem.* **2021**, *35*, 116061.
15. Krapf, M. K.; Gallus, J.; Wiese, M. *Eur. J. Med. Chem.* **2017**, *139*, 587-611.
16. Krapf, M. K.; Gallus, J.; Spindler, A.; Wiese, M. *Eur. J. Med. Chem.* **2019**, *161*, 506-525.
17. Jeminejs, A.; Goliškina, S. M.; Novosjolova, I.; Stepanovs, D.; Bizdēna, Ē.; Turks, M. *Synthesis* **2021**, *53*, 1443-1456.
18. Novosjolova, I.; Bizdena, E.; Turks, M. *Eur. J. Org. Chem.* **2015**, *2015*, 3629-3649.
19. Cīrule, D.; Ozols, K.; Platnieks, O.; Bizdēna, Ē.; Māliņa, I.; Turks, M. *Tetrahedron* **2016**, *72*, 4177-4185.
20. Novosjolova, I.; Bizděna, E.; Turks, M. *Tetrahedron Lett.* **2013**, *54*, 6557-6561.
21. Kavoosi, S.; Rayala, R.; Walsh, B.; Barrios, M.; Gonzalez, W. G.; Miksovska, J.; Mathivathanan, L.;

Raptis, R. G.; Wnuk, S. F. *Tetrahedron Lett.* **2016**, *57*, 4364-4367.
22. Jeminejs, A.; Novosjolova, I.; Bizdēna, Ē.; Turks, M. *Org, Biomol. Chem.* **2021**, *19*, 7706-7723.
23. Motoyama, M.; Doan, T. H.; Hibner-Kulicka, P.; Otake, R.; Lukarska, M.; Lohier, J. F.; Ozawa, K.; Nanbu, S.; Alayrac, C.; Suzuki, Y.; Witulski, B. *Chem. Asian J.* **2021**, *16*, 2087-2099.
24. Maluleka, M. M.; Mokoena, T. P.; Mampa, R. R. *J. Mol. Struct.* **2022**, *1255*, 132439.
25. DeLano, T. J.; Bandarage, U. K.; Palaychuk, N.; Green, J.; Boyd, M. J. *J. Org. Chem.* **2016**, *81*, 12525-12531.
26. Charaschanya, M.; Bogdan, A. R.; Wang, Y.; Djuric, S. W. *Tetrahedron Lett.* **2016**, *57*, 1035-1039.
27. Shen, C.; Wang, L.; Wen, M.; Shen, H.; Jin, J.; Zhang, P. *Ind. Eng. Chem. Res.* **2016**, *55*, 3177-3181.
28. Yang, Q.; Lou, M.; Yin, Z.; Deng, Z.; Ding, Q.; Peng, Y. *Org. Biomol. Chem.* **2018**, *16*, 8724-8731.
29. Yang, Q.; Yin, Z.; Zheng, L.; Yuan, J.; Wei, S.; Ding, Q.; Peng, Y. *RSC Advances* **2019**, *9*, 5870-5877.
30. Wisniewski, S. R.; Stevens, J. M.; Yu, M.; Fraunhoffer, K. J.; Romero, E. O.; Savage, S. A. *J. Org. Chem.* **2019**, *84*, 4704-4714.
31. Meesa, S. R.; Naikawadi, P. K.; Gugulothu, K.; Shiva Kumar, K. *Org. Biomol. Chem.* **2020**, *18*, 3032-3037.
32. Liu, X. Y.; Liu, H.; Liao, X. Z.; Dong, L.; Chen, F. E. *Adv. Synth. Catal.* **2020**, *362*, 5645-5652.
33. Samandram, R.; Korukçu, M. Ç.; Cośkun, N. *Synthesis* **2022**, *54*, 210-216.
34. Zhao, X.; Zhou, Y.; Yang, Q.; Xie, Y.; Ding, Q.; Deng, Z.; Zhang, M.; Xu, J.; Peng, Y. *Synthesis* **2013**, *45*, 3245-3250.
35. Peng, Y.; Huang, P.; Wang, Y.; Zhou, Y.; Yuan, J.; Yang, Q.; Jiang, X.; Deng, Z.; Xu, J. *Org. Biomol. Chem.* **2014**, *12*, 5922-5927.
36. Ye, X.; Yuan, Z.; Zhou, Y.; Yang, Q.; Xie, Y.; Deng, Z.; Peng, Y. *J. Heterocycl. Chem.* **2016**, *53*, 1956-1962.
37. Dhuguru, J.; Liu, W.; Gonzalez, W. G.; Babinchak, W. M.; Miksovska, J.; Landgraf, R.; Wilson, J. N. *J. Org. Chem.* **2014**, *79*, 4940-4947.
38. Achelle, S.; Rodríguez-López, J.; Robin-Le Guen, F. *J. Org. Chem.* **2014**, *79*, 7564-7571.
39. Kabri, Y.; Crozet, M. D.; Redon, S.; Vanelle, P. *Synthesis* **2014**, *46*, 1613-1620.
40. Soussi, M. A.; Provot, O.; Bernadat, G.; Bignon, J.; Desravines, D.; Dubois, J.; Brion, J. D.; Messaoudi, S.; Alami, M. *ChemMedChem* **2015**, *10*, 1392-1402.
41. Babu, D. S.; Srinivasulu, D.; Kotakadi, V. S. *Chem. Heterocycl. Compd.* **2015**, *51*, 60-66.
42. Ye, X.; Yuan, J.; Zhou, Y.; Deng, Z.; Mao, X.; Peng, Y. *Synthesis* **2016**, *48*, 3976-3984.
43. Qiu, G.; Huang, P.; Yang, Q.; Lu, H.; Xu, J.; Deng, Z.; Zhang, M.; Peng, Y. *Synthesis* **2013**, *45*, 3131-3136.
44. Pulipati, Y.; Gurram, V.; Laxmi, S. V.; Satyanarayana, Y.; Singh, K.; Kumar, V.; Sharma, S.; Pottabathini, N.; Iska, V. B. R. *Synth. Commun.* **2017**, *47*, 1142-1150.
45. Plaza-Pedroche, R.; Georgiou, D.; Fakis, M.; Fihey, A.; Katan, C.; Robin-le Guen, F.; Achelle, S.; Rodríguez-López, J. *Dyes Pigm.* **2021**, *185*, 108948.
46. Patel, A. B.; Rohit, J. V. *Polycycl. Aromat. Compd.* **2021**, 1970586.
47. Ye, X.; Huang, J.; Deng, Z.; Yuan, J.; Peng, Y. *Synthesis* **2021**, *53*, 383-390.
48. Ye, X.; Huang, J.; Deng, Z.; Peng, Y. *Synthesis* **2022**, *54*, 788-796.
49. Dos Santos, T.; Orenha, H. P.; Murie, V. E.; Vessecchi, R.; Clososki, G. C. *Org. Lett.* **2021**, *23*, 7396-7400.
50. Bozzini, L. A.; Dos Santos, T.; Murie, V. E.; De Mello, M. B. M.; Vessecchi, R.; Clososki, G. C. *J. Org. Chem.* **2021**, *86*, 1204-1215.
51. Murie, V. E.; Nicolino, P. V.; dos Santos, T.; Gambacorta, G.; Nishimura, R. H. V.; Perovani, I. S.; Furtado, L. C.; Costa-Lotufo, L. V.; Moraes de Oliveira, A.; Vessecchi, R.; Baxendale, I. R.; Clososki, G. C. *J. Org. Chem.* **2021**, *86*, 13402-13419.
52. Hess, A.; Alandini, N.; Guelen, H. C.; Prohaska, J. P.; Knochel, P. *Chem. Commun.* **2022**, *58*, 8774-8777.
53. Nishimura, R. H. V.; Murie, V. E.; Vessecchi, R.; Clososki, G. C. *ChemistrySelect.* **2020**, *5*, 11106-11111.

54. Hoffmann, N. *Chem. Rev.* **2008**, *108*, 1052-1103.
55. Crisenza, G. E. M.; Melchiorre, P. *Nature Commun.* **2020**, *11*, 803.
56. Yuan, Y.; Lei, A. *Nature Commun.* **2020**, *11*, 802.
57. Rattanangkool, E.; Sukwattanasinitt, M.; Wacharasindhu, S. *J. Org. Chem.* **2017**, *82*, 13256-13262.
58. Todorov, A. R.; Wirtanen, T.; Helaja, J. *J. Org. Chem.* **2017**, *82*, 13756-13767.
59. Dong, J.; Xia, Q.; Lv, X.; Yan, C.; Song, H.; Liu, Y.; Wang, Q. *Org. Lett.* **2018**, *20*, 5661-5665.
60. Wang, Z.; Dong, J.; Hao, Y.; Li, Y.; Liu, Y.; Song, H.; Wang, Q. *J. Org. Chem.* **2019**, *84*, 16245-16253.
61. Dong, J.; Lyu, X.; Wang, Z.; Wang, X.; Song, H.; Liu, Y.; Wang, Q. *Chem. Science* **2019**, *10*, 976-982.
62. Gao, Y.; Wu, Z.; Yu, L.; Wang, Y.; Pan, Y. *Angew. Chem. Int. Ed.* **2020**, *132*, 10951-10955.